SEED-BASED AND DATA-DRIVEN ANALYSES OF DEFAULT MODE NETWORK CONNECTIVITY MEASURES IN DEMENTIA

by

Başak Kılıç

B.S., Electrical Engineering, University of California, Los Angeles, 2010

Submitted to the Institute for Graduate Studies in
Science and Engineering in partial fulfillment of
the requirements for the degree of
Master of Science

Graduate Program in Systems and Control Engineering
Boğaziçi University

2017

SEED-BASED AND DATA-DRIVEN ANALYSES OF DEFAULT MODE NETWORK CONNECTIVITY MEASURES IN DEMENTIA

APPROVED BY:

Assoc. Prof. Burak Acar ..... (Thesis Supervisor)

Prof. Tamer Demiralp .....

Prof. Yağmur Denizhan .....

DATE OF APPROVAL: 10.01.2017

ACKNOWLEDGEMENTS

I firstly would like to express my sincere gratitude to my research advisor Dr. Burak Acar for his continuous support and encouragement. It has been an invaluable experience for me to work on the BRAINet project, during which I gained a tremendous amount of knowledge and had a chance to work with great scientists. I would like to thank each one of these great people, Dr. Tamer Demiralp, Dr. Hakan Gürvit, Dr. Aslı Demirtaş-Tatlıdede, Dr. Başar Bilgiç, Dr. Alkan Kabakçıoğlu, Dr. Evren Özarslan and Dr. Şule Yazıcı. I would also like to thank Dr. Ahmet Ademoğlu for his time and suggestions.

New starts are never easy, and the transition process requires daunting bravery, many hours of hard-work and never-ending motivation. I have had great mentors on this challenging journey, whose contributions I will always remember and remain grateful for. For this reason, I would like to thank Dr. Yağmur Denizhan, Dr. Fatoş Yarman-Vural, Dr. Banu Onaral and Dr. Kadri Özçaldıran for their mentorship, support and insightful suggestions that helped me start and complete such a journey.

Thanks to Çiğdem Ulaşoğlu, Elif Kurt, Tuna Çakar and Emre Kale for sharing their knowledge and experience, and Erhan Özacar for captivating physics discussions.

I am truly grateful to my family and friends that I consider part of the family for their never-ending unconditional love and trust. I would like to thank each one of them for teaching me about love, caring for one another, finding happiness in small things, believing in the magic of hard-work and living according to one's virtues while keeping family always as top priority.

This thesis was supported by TÜBİTAK ARDEB 1003 Programme grant #114E053 and Boğaziçi University Research Funds (BAP) grant #10520.

ABSTRACT

SEED-BASED AND DATA-DRIVEN ANALYSES OF DEFAULT MODE NETWORK CONNECTIVITY MEASURES IN DEMENTIA

Functional neuroimaging and its applications to neurodegenerative diseases and mental illnesses have created an enlarging area of interest that varying lines of research ranging from molecular biology to engineering contribute to. Among them, Alzheimer's disease has a critical importance by causing the largest number of dementia cases. Recently, mild and subjective cognitive impairments have also been associated with Alzheimer's as possible indicators of cognitive decline. Using resting-state fMRI to investigate functional connectivity measures and detect any abnormality within and between networks have yielded promising results that disclose information about the nature of the diseases. The objective of this thesis is to use varying resting-state fMRI methods to differentiate between SCI, MCI and AD patients by investigating the changes within Default Mode Network (DMN). The obtained results indicate that the changes within the functional connectivity measures among DMN components can be detected independent of the method of choice, and the measures of connectivity differ among groups. Subsequent research would aim for detection of possible bio-markers that are present through several stages and finding a common framework where metrics obtained from different methods can be compared.

ÖZET

DEMANSIN OLAĞAN DURUM ŞEBEKESİ ÜZERİNE ETKİSİNİN TOHUM-TABANLI VE VERİ-BAZLI ANALİZLER KULLANILARAK İNCELENMESİ

İşlevsel beyin görüntüleme metodları ve bu metodların nörodejeneratif ve zihinsel hastalıkların tanısında kullanılabilmesi geniş bir araştırma alanı oluşturmuş, moleküler biyolojiden mühendisliğe kadar geniş bir yelpazede yapılan çalışmaların bu alana katkıda bulunabildiği gözlenmiştir. Demans hastalarında en sık gorülmesi nedeniyle, Alzheimer's (AD) nörodejeneratif hastalıklar arasında önemli bir yere sahiptir. Son zamanlarda, hafif (MCI) ve öznel (SCI) bilişsel bozukluklar Alzheimer's ile karşılaştırılmakta ve bu bozuklukların Alzheimer's için bir ön tanı olarak kullanılabilirliği araştırılmaktadr. Dinlenme halinde çekilen işlevsel manyetik rezonans (MR) görüntülerinden elde edilen bilgiler ile, dinlenme halindeki ağlar ve bu ağları meydana getiren bölgeler arasındaki kimi bozulmalar, hastalığın nasıl ilerlediği üzerine önemli bulgular saptanabilmesine yardımcı olmuştur. Bu tezin amacı, çeşitli dinlenme hali işlevsel MR metodlarını kullanarak SCI, MCI ve AD hastalarına ait olağan durum şebekelerindeki bozulmaları ve bu bozulmaların nasıl farklılıklar gösterdiğini gözlemlemektir. Kullanılan metoda bağımlı olmaksızın, olağan durum şebekesini meydana getiren işlevsel bağlantıların bu üç grup arasında farklılıklar gösterdiği gözlenmiştir. Bundan sonra yapılacak araştırmalarda hedeflenen amaç, hastalık seyri boyunca geçişleri takip edebilmemizi sağlayacak biyolojik göstergelerin saptanması ve kullanılan farklı metodlardan alınan sonuçların, oluşturulacak ortak bir platformda değerlendirilmesi olacaktır.

TABLE OF CONTENTS

ACKNOWLEDGEMENTS iii
ABSTRACT iv
ÖZET v
LIST OF FIGURES vii
LIST OF TABLES x
LIST OF SYMBOLS xi
LIST OF ACRONYMS/ABBREVIATIONS xii
1. INTRODUCTION 1
1.1. Overview 1
1.2. Functional Magnetic Resonance Imaging 2
1.3. Functional Connectivity 4
1.4. Dementia 6
2. FUNCTIONAL MRI ANALYSIS 9
2.1. Preprocessing 9
2.2. Methods 10
2.2.1. Seed-Based Analysis 12
2.2.2. Independent Component Analysis 13
2.2.3. Cluster Analysis 15
3. EXPERIMENTS AND RESULTS 17
3.1. Subjects and Methods 17
3.2. Analyses and Results 18
3.2.1. Seed-Based Analysis 18
3.2.2. Independent Component Analysis 23
3.2.3. Cluster Analysis 32
4. DISCUSSION AND CONCLUSION 39
REFERENCES 44
APPENDIX A: APPLICATION 58

LIST OF FIGURES

Figure 1.1. Functional MRI (fMRI) uses the change in blood flow to detect areas with greater activity. 4

Figure 1.2. Resting state networks [1]. 6

Figure 1.3. AD pathological cascade model biomarkers [2]. 7

Figure 2.1. An overview of the pre-processing steps followed by the selected methods of analysis applied on the functional MRI data. 11

Figure 2.2. ICA is a blind source separation problem. 13

Figure 2.3. FMRI signals, here represented as measured signals, are decomposed as spatial maps and corresponding time courses [3]. 14

Figure 2.4. Vector-matrix representation for spatial ICA. 15

Figure 3.1. Four DMN components were selected as seeds for the seed-to-voxel analysis, which were PCC (Posterior Cingulate Cortex), MPFC (Medial Prefrontal Cortex), LLP (Left Inferior Parietal Lobe) and RLP (Right Inferior Parietal Lobule) [4]. 20

Figure 3.2. When AD patients were compared to SCI patients with PCC selected as a seed region. (a) Axial View. (b) Sagittal View. 22

Figure 3.3. When AD patients were compared to SCI patients with RLP selected as a seed region. (a) Axial View. (b) Sagittal View. 22

Figure 3.4. When MCI patients were compared to SCI patients with PCC selected as a seed region. (a) Axial View. (b) Sagittal View. 23

Figure 3.5. When MCI patients were compared to SCI patients with LLP selected as a seed region. (a) Axial View. (b) Sagittal View. 23

Figure 3.6. Component 6, spatial map and associated time course. 26

Figure 3.7. Component 12, spatial map and associated time course. 26

Figure 3.8. Component 13, spatial map and associated time course. 27

Figure 3.9. Component 22, spatial map and associated time course. 27

Figure 3.10. Component 29, spatial map and associated time course. 28

Figure 3.11. A comparison of the DMN related components, with their corresponding time courses. 28

Figure 3.12. T-map for Component 6. 29

Figure 3.13. T-map for Component 12. 30

Figure 3.14. T-map for Component 13. 30

Figure 3.15. T-map for Component 22. 31

Figure 3.16. T-map for Component 29. 31

Figure 3.17. Correlations for functional network connectivity among DMN related components. Correlations were calculated using spatial maps. 32

Figure 3.18. Cross-correlation of time series associated with DMN related components. 32

Figure 3.19. Silhouette coefficients contrast when Square Euclidean distance measure was used with random initialization. 35

Figure 3.20. Silhouette coefficients contrast when L1 distance measure was used with random initialization. 36

Figure 3.21. Silhouette coefficients contrast when Square Euclidean distance measure was used with k-means++ algorithm initialization. 36

Figure 3.22. Silhouette coefficients contrast when L1 distance measure was used with k-means++ algorithm initialization. 37

Figure A.1. Map of Broadmann [5]. 58

Figure A.2. Surface view of the human brain, LH [5]. 58

Figure A.3. Midsagittal view of the human brain, LH [5]. 59

Figure A.4. Ventral view of the human brain, LH [5]. 59

LIST OF TABLES

Table 3.1. Seed-to-Voxel Analysis Result Table. Differences in functional connectivity measures between SCI, MCI and AD groups at cluster level. 21

LIST OF SYMBOLS

a_{ij}	Mixing coefficients
$\mathbf{A}$	Mixing matrix
$\mathbf{C}_k$	Cluster centroid
$\mathbf{d}_{x,j}$	Distance between observation and centroid
$\mathbf{H}$	Entropy
$\mathbf{I}_W$	Within-cluster inertia
$\mathbf{I}_B$	Between-cluster inertia
$\mathbf{s}$	Source signals
$\mathbf{W}$	Unmixing matrix
$\mathbf{x}$	Observed Signals
$\mathbf{y}$	Extracted Signals
$\mathbf{z}$	Voxel value
Ω_x	Voxels in seed area

LIST OF ACRONYMS/ABBREVIATIONS

3D	Three Dimensional
4D	Four Dimensional
AD	Alzheimer's Disease
CDF	Cumulative Density Function
CSF	Cerebrospinal Fluid
DMN	Default Mode Network
DMPFC	Dorsomedial Prefrontal Cortex
EEG	Electroencephalography
FDR	False Discovery Rate
FMRI	Functional Magnetic Resonance Imaging
FWER	Family-wise Error Rate
FWHM	Full-Width-Half-Maximum
GM	Gray Matter
HF+	Hippocampal Formation
ICA	Independent Component Analysis
LLP	Left Inferior Parietal Lobe
LTC	Lateral Temporal Cortex
MCI	Mild Cognitive Impairment
MEG	Magnetoencephalography
MNI	Montreal Neurological Institute
MPFC	Medial Prefrontal Cortex
MTL	Medial Temporal Lobe
NIRS	Near Infrared Spectroscopy
PCA	Principal Component Analysis
PCC	Posterior Cingulate Cortex
PET	Positron Emmision Tomography
PHC	Parahippocampal Cortex
RLP	Right Inferior Parietal Lobe

ROI	Region-of-Interest
SCI	Subjective Cognitive Impairment
SICA	Spatial ICA
SNR	Signal-to-Noise Ratio
TICA	Temporal ICA
VMPFC	Ventromedial Prefrontal Cortex
WM	White Matter

1. INTRODUCTION

1.1. Overview

Brain is a huge and complex network that consists of several sub-networks working with each other and against each other for any given task. Regardless of its complexity, its efficiency and dynamic structure make brain an interesting structure of networks that allows different regions to work together even though they are anatomically separated. Functional neuroimaging can be defined as an approach to understand brain activity and corresponding physiological changes that are detected by a set of techniques [6]. There are several methods that are used to understand the patterns of activity created by temporal correlations of separate brain regions [7]. Each functional neuroimaging method is characterized by its temporal and spatial resolutions besides the implementation of the method itself.

Functional magnetic resonance imaging (fMRI) is a functional neuroimaging method, which can be used for both task-based and task-free analyses. Both approaches are frequently used depending on the nature of the experiment [5]. The first task-free or rs-fMRI analysis took place after realization that the brain was not idle during rest, which was thought to be the case until 1980s. As the measurements indicated, there was an ongoing communication between brain regions and, the energy consumption during rest was as high as during task related activities [8, 9]. The first resting state fMRI analysis was conducted by Biswal *et al.*, who were able to measure low frequency fluctuations in sensorimotor cortex [8].

In recent years, many researchers have started using neuroimaging methodologies for understanding changes in brain connectivity, caused by neurodegenerative and mental diseases [10]. The motivation behind these works is not only finding a cure for the diseases such as Alzheimer's or Parkinson, but also slowing down and monitoring the disease progress. Among all resting state networks that have been studied through rs-fMRI, Default Mode Network holds an important place since it has been constantly

marked with functional changes [11]. In the case of Alzheimer's disease, which is considered to be the most common form of dementia today [12], functional connectivity measures among DMN components and the network's connection to other resting-state networks show significant differences when compared to healthy controls [13].

The main motivation behind this work is to understand the changes of functional connectivity measures within the components of Default Mode Network for people suffering from dementia. The analyses are conducted on three subject groups: subjective cognitive impairment (SCI), mild cognitive impairment (MCI) and Alzheimer's disease (AD). SCI patients differ from MCI and AD patients since they suffer from cognitive complaints that lack neurological reasoning [14]. MCI, on the other hand, has already been reported in follow-up studies to turn into AD, with annual rate of 10-15% [15, 16]. In the subsequent sections, functional neuroimaging as a concept and functional connectivity analysis as an approach will be presented. The last section will focus on dementia and previous work that used functional neuroimaging methods to detect changes within and between functional brain networks for dementia related diseases, with several conditions and varying stages. Other neurodegenerative and mental diseases that suffer from functional connectivity disruptions, especially in DMN, have been included as additional references. Chapter 2 will present information about the fMRI analysis methods that are currently used through providing information about the processing of fMRI data and method selection processes. Chapter 3 will present experimental results with accompanying information about the subjects and methods of selection. Chapter 4 will consist of discussion of the results and conclusion of the study.

1.2. Functional Magnetic Resonance Imaging

Instead of measuring neuronal activity directly such as through changes in electrical potentials, functional MRI measures neuronal activity indirectly by using metabolic changes, such as blood oxygenation level, that are generated by the underlying neuronal activity [5]. The so-called neuronal activity that is generated by the change in MR signal is known as the haemodynamic response (HR). Electroencephalography

(EEG) and magnetoencephalography (MEG) are frequently used methods in addition to functional magnetic resonance imaging (fMRI) and positron emission tomography (PET) even though they differ in their temporal and spatial characteristics. EEG is able to capture the neural activity in a relatively shorter time, about 10-100 msec since it is an electrophysiological method [6]. On the other hand, because fMRI measures neural activity indirectly thru haemodynamic changes, it is slower compared to EEG; however, it gives better spatial resolution. Near infrared spectroscopy or NIRS is a type of optical imaging method that is similar to fMRI in terms of measurement, i.e. it uses cortical blood flow for measurement. However, it is not as widely accepted in spite of its ease of use since its resolution, both spatially and temporally, is not compatible with the already existing methods [6].

The brain consumes up to 20 percent of the energy generated in total, and in contrast to the early assumption that it is idle during rest, it consumes significant amount of energy even in resting state [9]. The energy used for the brain is generated from the oxidation of the glucose, which requires constant use of oxygen and glucose [6]. The process uses increased blood flow as a supply mechanism, which displaces deoxyhemoglobin molecules with oxygenated hemoglobin, resulting in an increase in MR signal locally due to the difference between magnetic characteristics of the oxygenated and deoxygenated hemoglobin [5]. The level of present deoxygenated hemoglobin within a voxel is represented by the corresponding BOLD signal. Figure 1.1 gives an overview of the process and resulting BOLD contrast.

The main assumptions for characterizing the BOLD fMRI response are the area and the measure of neuronal activity [6]. BOLD fMRI measurements focus on the gray matter, where the synapses can be observed, rather than the white matter. Secondly, neuronal activity is not directly measured since the measurements are based on the output of synaptic activity, which leads to information about the neuronal activity. The fMRI analysis can be conducted in two ways: task-based or task-free. While task-based fMRI analyses have been around longer than task-free ones, task-free or resting state approach has also been adopted by many. The focus of resting-state fMRI experiments is the low frequency oscillations of time-series, which is approximately between 0.01

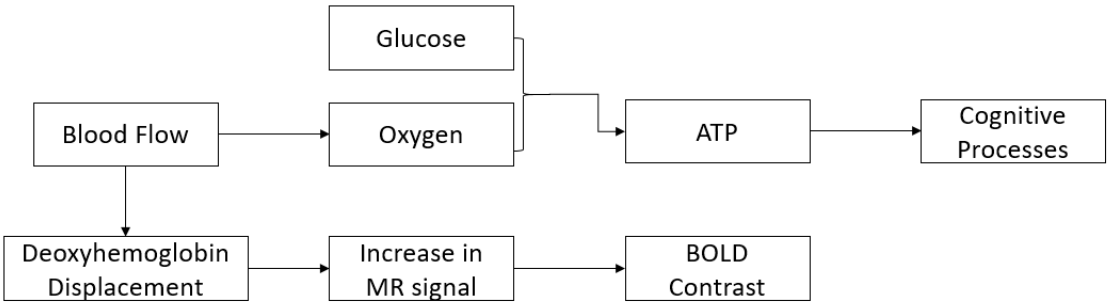

Figure 1.1. Functional MRI (fMRI) uses the change in blood flow to detect areas with greater activity.

Hz and 0.1 Hz [17]. During rs-fMRI scanning sessions, patients are instructed to relax and not to think of something particular while their eyes are open. Some studies state that keeping eyes open or close, or following instructions during rest state might be indicative of the fluctuations in measurements [18, 19]. An fMRI session is composed of low-resolution images that are taken few seconds apart. Images, which are also called volumes, compose of voxels, which are three dimensional structures that allow processing of the data. Each voxel is associated with a time series. Analyzing fMRI data is based on measuring the activation level of these voxels, which exhibit varying intensity levels at each time point. Functional connectivity measures are constructed on the information retrieved from voxel level activations.

1.3. Functional Connectivity

Functional connectivity describes the statistical patterns of neuronal activation among brain regions that are anatomically separated [7, 11]. As an initial step, a functional connectivity analysis consists of finding a set of nodes and, edges that connect these nodes [20]. Nodes, between which the connectivity measures are calculated, can be determined through several methods. These methods can be broadly categorized as model-based or data-driven. Seed-based analysis is an example of model-based methods whereas independent component analysis (ICA), principal component analysis (PCA), singular value decomposition (SVD), graph methods and clustering are examples of

data-driven methods. In seed-based analysis, node selection process requires a priori knowledge, which can be established through use of functional or anatomical mapping. In contrast, data-driven methods do not depend on a priori knowledge about the regions of interests. Data-driven analyses consist of finding functional connectivity measures among regions that are retrieved through processing of data. The next step in the analysis involves computing the functional connectivity measures among regions, mostly using time courses associated with each region. Full- and partial correlation, coherence, regularized inverse covariance and mutual information are some of the methods that are used to obtain these functional connectivity measures [20]. Learning more about the functional organization and communication among the brain regions provides new insights on cognitive processes and human behavior, which would eventually change our approach on how to analyze the information we have. Disruptions in resting state networks, for example, have been studied to understand the nature of neurodegenerative diseases such as Alzheimer's disease (AD), schizophrenia, and depression. Increasing disruptions in functional connectivity, particularly within the Default Mode Network have been shown for AD patients [21–23]. Among all the resting state networks, Default Mode Network (DMN) is the most frequently studied resting state network because the components of DMN exhibit high level of connectivity, both functionally and anatomically [24, 25]. The identification of DMN was first established by Raichle *et al.* on data acquired using PET, which was followed by works on understanding the nature of resting state as a whole [26, 27]. Subsequent identification of DMN by using fMRI was achieved by Greicius *et al.* [28]. Besides DMN, researchers were able to observe and identify other resting state networks, which are somatomotor, frontoparietal control, visual, language, dorsal attention and ventral attention networks [10, 22].

When conducting a functional connectivity analysis, it is essential to be able to detect noise sources and include them in the regression analysis prior to investigating functional connectivity. To eliminate artifacts, which are possibly caused by head movement or physiological effects generated by respiratory or cardiovascular systems, one can apply several pre-processing steps to the data of interest. These pre-processing steps can be applied in many ways with vast amount of processes and order of applications available even though some specific pipelines are adapted widely, such as the ones

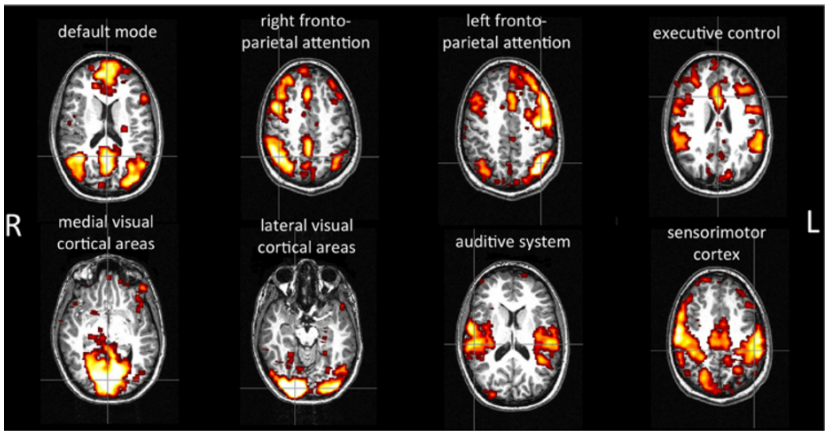

Figure 1.2. Resting state networks [1].

regarding spatial pre-processing. Besides spatial pre-processing, one can work on the temporal aspect of data. Other pre-processing methods, which are not yet settled in a common frame, include regression of global signal or, white matter and cerebrospinal fluid based regressors [29]. As some of these steps are reported to have no effect on the connectivity analysis, some are still accepted as essential parts of the analysis as a whole [30]. The following sections contain more detailed information on the application of these pre-processing steps and how frequently they are used.

1.4. Dementia

Dementia is a set of symptoms that is associated with memory impairments and difficulty in thinking clearly. Many people that have dementia suffer from Alzheimer's disease (AD) since AD is claimed to cause most of the dementia cases and considered to be one of the most common and lethal diseases of our times [12]. Currently, there are not any treatments available to cure the disease. In addition to research on possible cures, there are on-going research that focus on finding treatment methods to slow down the progress of the disease by early detection of possible biomarkers [31]. Some of these biomarkers are aimed to be detected through imaging methodologies and others involve analysis of neurochemical entities such as amyloid beta peptides, tau and hyper-phosphorylated tau (p-tau) proteins [32, 33].

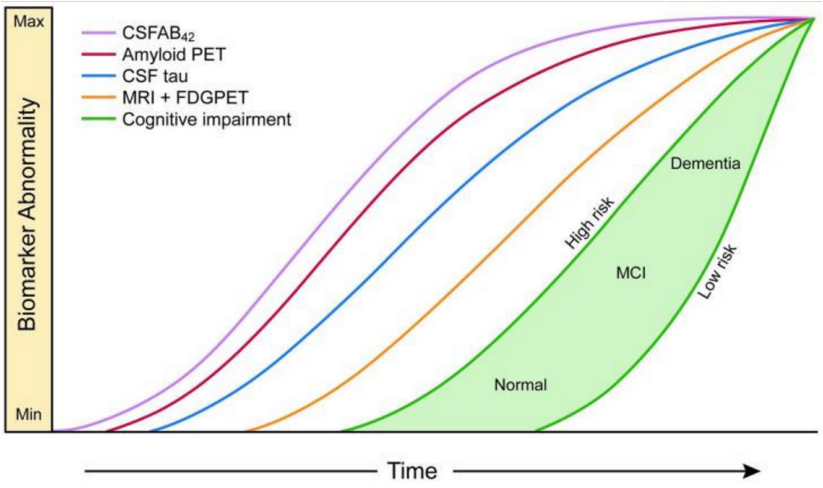

Figure 1.3. AD pathological cascade model biomarkers [2].

As neuropathology led information constitute an important aspect of the research on biomarkers, the neuroimaging methods also have contributed critical insights for the research purposes. Most dominant characteristics that have been identified through the use of imaging methods are the change in the volumetric structure and, deformations in the structural and functional connectivity measures of the brain. In AD, specifically, apparent deformations within medial temporal, posterior cingulate, precuneus, and lateral temporoparietal areas can be seen in addition to cognitive incapacities [34]. As a general pattern, the disease first affects a small area in the brain, which later enlarges as synapses weaken, and as a result the symptoms worsen. In a group ICA analysis, Damoiseaux et al. reported that in a longitudinal Alzheimer's study, follow-up results indicated significantly decreased functional connectivity compared to baseline after gray matter density correction [15]. In addition to Alzheimer's, there are several other illnesses that might benefit from the findings of neuroimaging methods. Neurodegenerative diseases such as Parkinson's disease and amyotrophic lateral sclerosis (ALS) or, mental diseases such as schizophrenia and depression can be given as examples [35–43] as discoveries about neurological underlying of some syndromes are continuously disclosed, and the use of neuroimaging methods are widely accepted with repeatable and reliable results [10]. In the case of dementia, the scope of the research interests using functional connectivity measures widens since it consists of stages and symptoms that

can occur in many diseases under different conditions and severities. Some of research focus on the area of analyzing normal aging and corresponding cognitive decline by using fMRI [23, 44–46], while others investigate the possible future connectivity disruptions in subjective cognitive impairment [14, 47]. Alzheimer's disease (AD) and its progression [48–50] is particularly a prominent area where most of the research is done in addition to mild cognitive impairment (MCI) [51–54] and its relation to AD [13,55]. Since Alzheimer's disease does not have a cure yet, it is important to detect and subsequently investigate biomarkers that would allow prevention and early detection of the disease [32, 56–63].

Even though there are not assured claims about the certain effects of Alzheimer's disease on functional network dysfunctions, there are piling work that showcase decrease functionality of networks through some specific regions that are targeted for people with no sign of AD, but with high amyloid burden [46,62]. Additionally, changes within the functional connectivity measures of the hippocampus makes it an important biomarker to AD [61]. Default Mode Network is one of the most analyzed resting state networks for neurodegenerative diseases due its structural and functional characteristics that might reflect the strength of functional connectivity measures within [64]. Hence, functional connectivity analysis of Default Mode Network (DMN) has been an important aspect of research questions that focus on finding an early biomarker for Alzheimer's disease [65]. Its investigation spans both the changes within the network and how its connection to remaining networks differ throughout the progression of the disease. Besides, the disease progression and its effects on DMN and its components lead to important information about the nature of the disease and its possible implications. The abnormal pattern of activity indicating disruptions in functional connectivity among DMN structures point out decreased connectivity measures in MCI and AD patients, while some other studies report increased connectivity with some regions that they frame as abnormal [15, 23, 53, 65–69].

2. FUNCTIONAL MRI ANALYSIS

2.1. Preprocessing

Independent of the choice of methodology, there are several pre-processing steps that have been applied prior to connectivity analyses. Even though there is not any specific or universal pipeline for pre-processing the fMRI data, there exists some agreements on the types of available processes in suggestion. These pre-processing steps can be summarized as, note that the order of the processes is preferential, slice-timing correction, realignment, co-registration, smoothing, normalization and temporal filtering. Slice-timing correction is applied for adjusting the time differences among slices of a volume. The data is adjusted generally by taking the first or the middle slice as the reference slice since each slice is acquired at a different time. Realignment is applied for motion correction that may be generated by factors such as head motion, and the process uses rotation and translation values for transformation of the images. Co-registration is an important step which involves registering functional images to anatomical images. Smoothing is applied for reducing noise by using a Gaussian kernel, generally between 4 – 8 mm at half of the maximum value, or FWHM. Normalization is useful and necessary when analyzing group fMRI data. Group fMRI analysis requires consideration of the fact that size and shape of the brain is different for each individual, and hence a normalization step is applied to all data to minimalize these differences by using a common template. Temporal filtering is used to increase SNR by removing noise sources generated by physiological effects. Generally low-pass and band-pass filters are preferred while applying temporal filtering. Besides, there are some additional nuisance regression steps such as use of white matter and cerebrospinal fluid (CSF) based regressors, or global signal regression, which is debated over introducing anti-correlations to data [4, 10, 29, 70].

2.2. Methods

There are various methods that have been largely used to process fMRI data such as seed-based methods, independent component analysis (ICA), principal component analysis (PCA), singular value decomposition (SVD), graph methods, pattern classifiers and several clustering methods such as hierarchical, k-means and spectral clustering algorithms. Seed-based methods, which are model-dependent, are the most commonly used methods due to their straight-forward application and their results' ease of interpretability. In seed methods, a region-of-interest (ROI) is selected and its time series is correlated with the time series of other regions. The resulting correlation matrices constitute a functional connectivity map, which displays how functionally connected is the region that is used as a seed to another region or the rest of the brain. Working with a region of interest provides an easy way to interpret results; however, the same advantage turns into a disadvantage while considering whole brain connectivity since the analysis is constrained by the selected region of interest and its comparison to the remaining parts of the brain. Hence, seed methods are much more convenient and informative while examining the measure of functional connectivity of a specific brain region rather than measuring the connectivity for the whole brain.

There are also data-driven methods such as principal component analysis (PCA), independent component analysis (ICA), singular value decomposition (SVD) and clustering. The main difference between data-driven, or model-free, and seed methods is that data-driven methods do not require a priori knowledge. As seed methods focus on a specific region (region-of-interest) and how this region is functionally linked to other regions, data-driven methods examine the whole brain without attributing any importance to a specific region. Independent component analysis (ICA) is probably the most frequently used method among them due to its repeatable accuracy [11]. Unlike seed methods, which are not as effective for displaying overlapping networks, ICA can be applied to whole-brain data. The results from an ICA decomposition can be used to identify resting state networks that are overlapping. Another advantage of ICA is its use for removing artifacts that are generated by head motion and, respiratory and physiological effects such as breathing and cardiac pulsation. Hence, independent

component analysis proves to be a powerful approach by providing information about brain regions that are functionally independent even though overlapping of regions is not restricted [71].

Clustering is another data-driven method that has been applied to fMRI data successfully. Clustering works by using the similarity of data points; as data points displaying high level of similarity are clustered together while seeking minimum level of similarity between data points that belong to different clusters. K-means, hierarchical and spectral clustering can be given as examples for some of the most commonly used clustering algorithms. It is interesting to note that regardless of the method of choice, both seed based and data driven methods, such as ICA or clustering, lead to similar results [11]. An overview of the pre-processing steps followed by the selected methods of analysis applied on the functional MRI data is displayed on Figure 2.1.

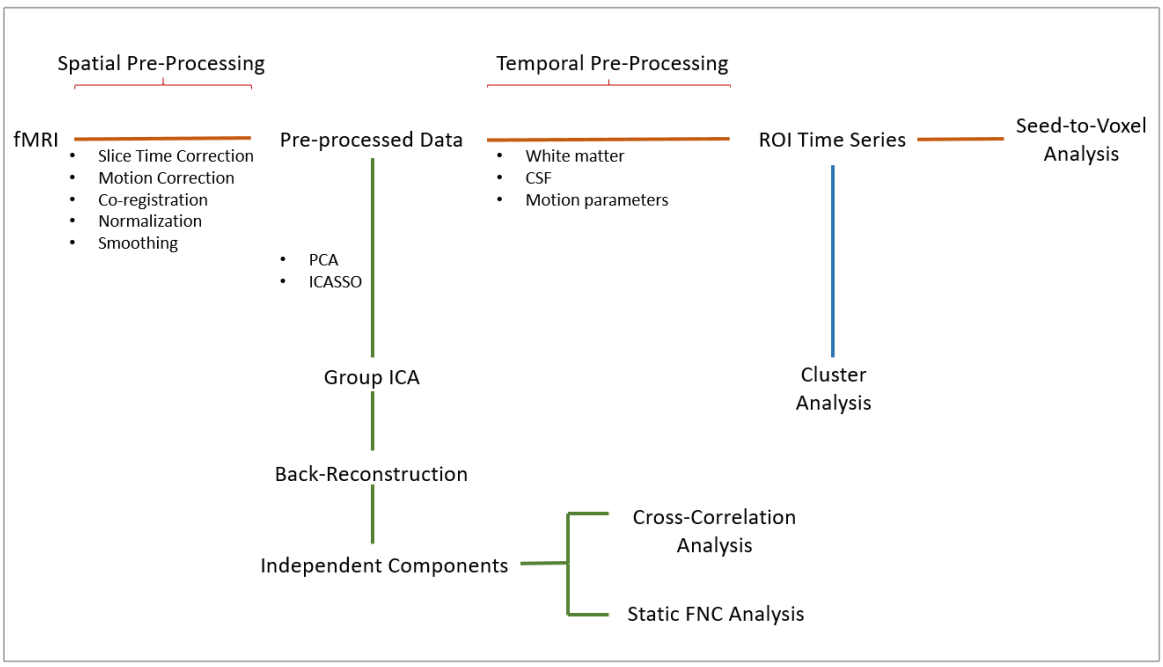

Figure 2.1. An overview of the pre-processing steps followed by the selected methods of analysis applied on the functional MRI data.

2.2.1. Seed-Based Analysis

Seed-based analysis is an approach for analyzing functional connectivity between specific regions. Also named as region-of-interest (ROI) analysis, one can test the statistical connection between groups of voxels. Seed-based analysis is particularly important when a specific anatomical brain region is under investigation [5]. It is important to note that the voxels selected for the ROI analysis are treated as a homogeneous single unit. ROIs can be selected by using anatomical or functional information. Anatomical ROIs are selected by either using anatomical images or specific brain regions that are under investigation. Functional ROI selection process involves use of tasks to activate voxels in a specific area, which is then used as a region of interest [5].

The advantages of the analysis make seed-based approach a frequently applied method. The most important advantage of a seed-based approach is the simplicity it offers in terms of usability and the inference of the results. Since regions are pre-selected and there is indeed a hypothesis about the connectedness between those regions, one can interpret the outcome easily. A region-of-interest is taken as a single unit where all voxels that are part of the region contribute to it in terms of signal quality, resulting in an increase in signal to noise ratio (SNR) [5]. Another advantage is due to the limited area of investigation since few ROIs requires fewer number of statistical tests compared to whole-brain analysis; therefore, controlling for false positives [72].

The biggest disadvantage of seed-based analysis is that it requires pre-assumptions such that the regions under investigation shall be selected prior to the analysis. Another disadvantage is that the result of a single ROI-to-ROI analysis contains information only about the connectedness of these two regions. Evaluating the connectedness on a whole-brain level would be ineffective and prone to include more false positives. In comparison, the data-driven methods such as independent component or clustering analysis do not depend on any assumptions since they do not require any brain region to be selected for the analysis. As a result, their outcomes can be used for interpreting the connectedness among the brain regions without any exclusion.

2.2.2. Independent Component Analysis

Independent Component Analysis (ICA) is a powerful and effective data-driven method that has been frequently used to analyze functional MRI data. In broad terms, ICA is a method for solving the blind source separation (BSS) problem [73]. The cocktail party problem, which is a well-known analogy for the description of the blind source problem can be given as an example to explain how ICA is used for an fMRI analysis. The cocktail party problem constitutes two important elements, which are the source and mixed signals. Source signals are generated by the speakers, where each speaker contributes to the mixed signal in some amount that is defined by the physical distance of that source. ICA is used here to separate the source signals from the mixed signals that they generate. When applied to an fMRI data, its results can be used to differentiate between functionally connected regions. The analysis can be carried out either for a single or a group of subjects, and when it is applied to multiple subjects in a group, it is important to consider that the spatial maps and time courses will differ depending on the individual, which will require a specific group ICA approach [74, 75].

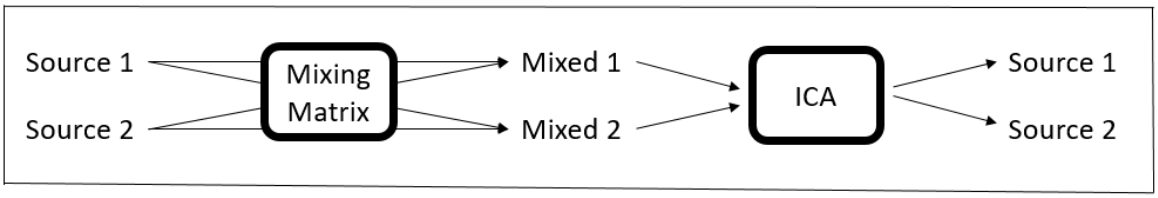

Figure 2.2. ICA is a blind source separation problem.

In order to recover source signals from signal mixtures, characteristics of signal features such as independence, normality and complexity are used. While applying ICA, only two of the characteristics are used, which are independence and normality [71]. The term independence, which is the most essential basis of the ICA analysis, is used to describe the statistical independency of signals. Since the source signals are independent, one can use this information to extract source signals from the signal mixtures since signal mixtures are composed of source signals, hence not independent.

The concept of normality is used to describe how gaussian or normal the signal is. As signal mixtures are less peaky than the source signals they are made of, they can be differentiated from their source signals by using the information retrieved from their relative histograms.

Despite the similarities between PCA and ICA, they differ fundamentally as PCA finds a set of signals that are uncorrelated to each other whereas the signals extracted by ICA are statistically independent. Due to independence constraint and its ability to represent the original data in smaller dimensions, PCA is generally used for pre-processing while working on fMRI data. ICA is easily applicable on the fMRI data if the number of source signals are equal to the number of mixed signals. On the other hand, if the number of mixed signals are greater than the number of source signals, one can apply PCA to data in order reduce the number of recovered signals.

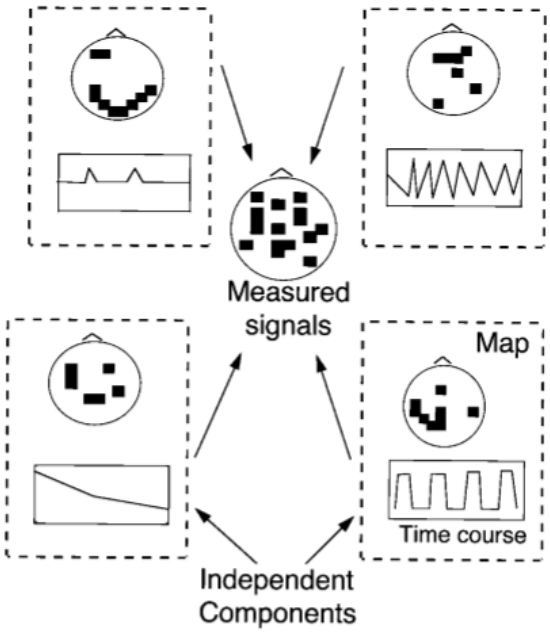

Figure 2.3. FMRI signals, here represented as measured signals, are decomposed as spatial maps and corresponding time courses [3].

When applied to rs-fMRI data, ICA decomposes the measured fMRI signal into independent components (IC), each of which is composed of a spatial map that discloses

the distribution of voxel values and a corresponding time course that depicts the information about activation. Each component can be an identifier of a different underlying neural process as well as a source of physiological or respiratory effect. Even though the analysis of spatial maps is an essential step for investigating functional connectivity, information retrieved from temporal components through time course analysis of networks yield to equally important insights [65]. For the purpose of the study, spatial ICA is preferred over temporal ICA for investigating within network connectivity between DMN components. Essentially, they both use the same algorithm for extracting source signals; however, spatial ICA (sICA) looks for independence among spatial sources while temporal ICA (tICA) looks for independence among temporal signals.

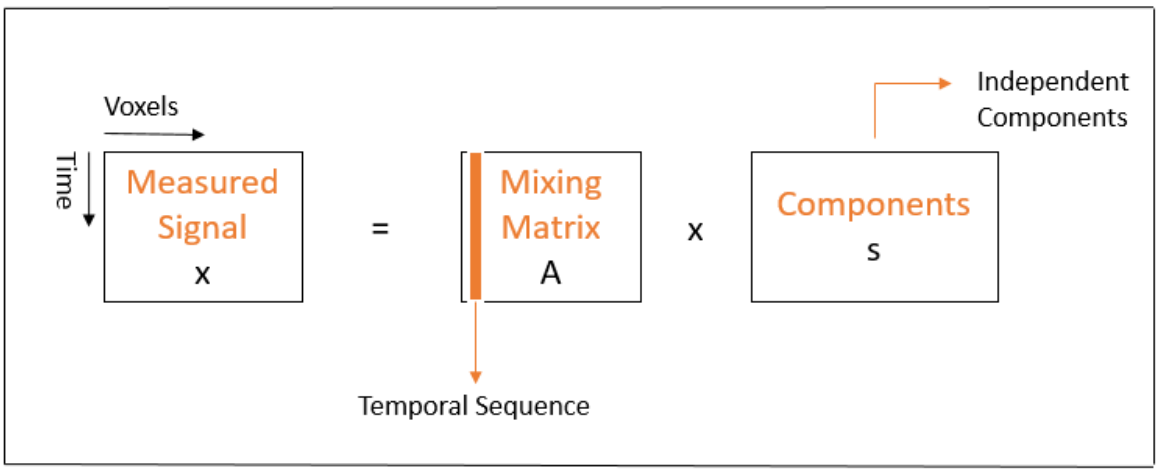

Figure 2.4. Vector-matrix representation for spatial ICA.

2.2.3. Cluster Analysis

The main advantage of clustering, which is also the main advantage for any data-driven method, is that it does not require any pre-assumptions about data. Additionally, it provides a selection mechanism that ICA lacks since results of an ICA analysis need to be examined either manually or through automatized processes to distinguish meaningful results from artifacts or noise [71, 76]. Clustering is used to partition data sets into groups based on their similarity measures. The algorithms can

be grouped under several headings, such as partitioning, hierarchical and density-based methods [77]. In general, all clustering algorithms can be defined as an optimization problem that has an objective function to be met. The aim is to differentiate data points, or observations, according to their within-group similarities and between-group dissimilarities. These differentiated data points are put into clusters, where data points within each of these clusters are the most similar. Conversely, one expects the data points in different clusters to be the most dissimilar. Hence, for any cluster analysis method, the main objective is to minimize the within-class inertia, or in other words, to maximize between-class inertia [78].

K-means is one of the partitioning methods that is based on assigning a group of objects, or data points, to k clusters based on the within-class and between-class measures. It is a relatively straight-forward algorithm that has been preferred by many. One of the biggest disadvantages of K-means is that the number of clusters has to be determined prior to analysis. Another factor to be taken into account while conducting such analysis is that both initialization and distance function have a high impact on the results, and preferred methods for choosing an initial cluster or similarity metric yields different results. In the case of fMRI data, this process consists of clustering the time courses of voxels based on their similarities. Clusters can be created by averaging the time course, either on a ROI level or by using all the time courses that belong to that cluster [78]. For fMRI data, it is also essential to identify and differentiate between non-active and active voxels, and compute clustering on the specific area since clustering results can be spread across whole data regardless of voxel activation level [79].

3. EXPERIMENTS AND RESULTS

3.1. Subjects and Methods

Functional and structural data were collected from 23 participants subject to Subjective Cognitive Impairment (10), Mild Cognitive Impairment (8) and Alzheimer's Disease (5). Imaging was performed on PHILIPS Achieva 3T X with a maximum 40 mT/m gradient strength and a maximum 200 mT/m/ms slew rate with a 32-channel head coil. The resting state fMRI were collected with single-shot EPI, using Fast Field Echo (FFE) technique on MS mode, with TE = 30 ms, TR = 3s, flip angle = 80 degrees, slice thickness = 3.31 mm, matrix size = 64x64, voxel size = 3.31mm x 3.31mm x 3.31mm, FOV RL = 212 mm, FOV AP = 199 mm, FOV FH = 159 mm. Total scan duration was 10 min, 3 s in duration (200 volumes). T1-weighted images were acquired with 3D Fast Field Echo (FFE) pulse sequence with multi shot Turbo Field Echo (TFE) imaging mode. The parameters were TE = 3.8 ms, TR = 8.3 ms, flip angle = 8 degrees, SENSE reduction 2 (Foot-Head) and 1 (Anterior-Posterior), FOV RL = 220 mm, FOV AP = 240 mm, voxel size = 1.0 mm x 1.0 mm x 1.0 mm, with factor of TFE 230 and the number of TFE shots 126. The spatial preprocessing pipeline was implemented using SPM12 [80] on Matlab (R2016a). For each participant, several pre-processing steps were applied to the functional images, which were slice-time correction, realignment, co-registration to anatomical image, normalization based on the Montreal Neurological Institute templates (MNI-152) and smoothing with a 6-mm Gaussian kernel. Additionally, the anatomical images were segmented into gray matter, white matter and cerebrospinal fluid (CSF) maps, the latter two of which were used for removal of confounding factors besides estimated motion parameters from the realignment step that were used as covariates.

3.2. Analyses and Results

3.2.1. Seed-Based Analysis

The seed-based resting state fMRI analysis was conducted using the CONN toolbox [81]. All the pre-processed data went under noise regression prior to the analysis. After applying white matter and CSF regression using aCompCor strategy [82] to the spatially pre-processed data, the noise reduction step was finalized by applying band-pass filter ($0.008Hz < f < 0.09Hz$) on the resulting time series. The seed-to-voxel analysis was conducted by calculating the Pearson's correlation coefficients between the time course of the seed and all other voxels, and applying Fisher's transformation to the correlation coefficients prior to group level analysis. To compute ROI time series from each seed area [4], the following Equation 3.1 was used, where BOLD timeseries at voxel v, voxels in seed area and time represented as BOLD(v,t), omega and t, respectively. m and n stand for the order of PCA component and temporal derivative, respectively:

$$\mathbf{x}_{n,m}(t) = \sum_{v \in \Omega_x} \mathbf{w}_m(v) \frac{\partial^n}{\partial t^n} BOLD(v,t) \tag{3.1}$$

The second level analysis was conducted to investigate functional connectivity measures such as the correlation or regression coefficients, and compare them among groups [4, 83]. Zero-lagged bivariate correlation coefficients, which presented information about the linear relation between BOLD time series of selected regions, were selected for measuring the functional connectivity between two regions [4]. Bivariate correlation coefficient defined as [4]:

$$\mathbf{r} = (\mathbf{x}^t\mathbf{x})^{\frac{-1}{2}}(\mathbf{x}^t\mathbf{y})(\mathbf{y}^t\mathbf{y})^{\frac{1}{2}} \tag{3.2}$$

where x and y stand for the BOLD time series of the source and target regions, respectively. Prior to group analysis, Fisher's transformation was applied to the correlation coefficients for transforming correlation coefficients to normally distributed scores. It is formulated as:

$$\mathbf{z}' = (0.5)(\ln(1+r) - \ln(1-r)) \tag{3.3}$$

DMN is more of a heterogeneous network than homogeneous, composed of two main sub-networks, namely PCC and MPFC [19, 84]. Four DMN regions, namely Posterior Cingulate Cortex (PCC), Medial Prefrontal Cortex (MPFC), Left Inferior Lobule (LLP) and Right Inferior Lobule (RLP) with MNI coordinates (0, -56, 28), (0, 54, -8), (-42, -68, 38) and (48, -60, 38) respectively, were chosen as seed regions. The SCI group versus the AD group, the SCI group versus the MCI group and the MCI group versus the AD group interactions were tested. The seed-to-voxel connections were tested for significance on a cluster-extent based threshold for a FWER (Family-wise Error Rate) correction. In comparison to voxel-level inference, which was used to detect voxels above some pre-determined threshold, cluster-extent based thresholding was used for determining a group of voxels forming a cluster, whose statistic values measured at voxel-level exceed a pre-determined threshold. Before measuring a cluster-level extent threshold, an arbitrary voxel-level threshold was applied to determine suprathreshold voxels that form clusters. Then, contiguous voxels were measured to detect whether any of the voxels in a cluster had not been activated according to the null hypothesis. Family-wise error rate (FWER) correction was applied to detect false positives since it gave the probability of at least one false positive under the null

hypothesis.

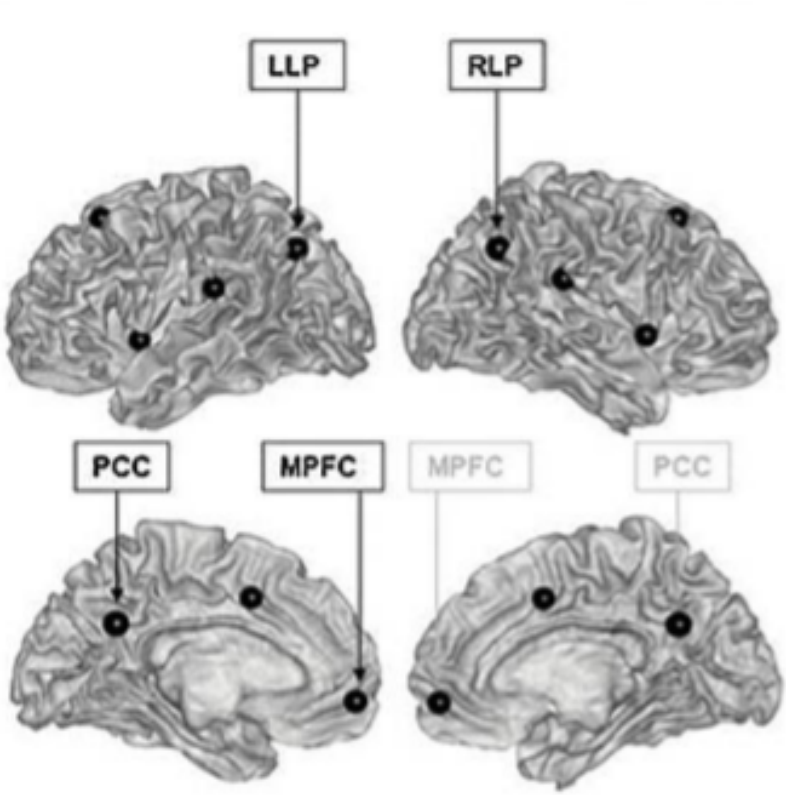

Figure 3.1. Four DMN components were selected as seeds for the seed-to-voxel analysis, which were PCC (Posterior Cingulate Cortex), MPFC (Medial Prefrontal Cortex), LLP (Left Inferior Parietal Lobe) and RLP (Right Inferior Parietal Lobule) [4].

Between-group t-tests were conducted to investigate differences between the SCI, MCI and AD groups. Two-sample t-tests revealed that both patients with AD and MCI displayed decreased connectivity compared to SCI patients. When AD patients were compared to SCI patients with PCC selected as a seed region, decreased connectivity in middle frontal gyrus and right superior frontal gyrus (height threshold $p < 0.001$; cluster-level FWE-corrected p = 0.043; peak (MNI) coordinates: 24, 46, 2) and, right middle frontal, right precentral and inferior frontal gyri (height threshold $p < 0.001$; cluster-level FWE-corrected p = 0.048; peak (MNI) coordinates: 40, 8, 44; see Table 3.1 and Figure 3.2) were observed. Additionally, AD patients showed

decreased connectivity in left superior and middle temporal gyrus (height threshold $p < 0.001$; cluster-level FWE-corrected p = 0.033; peak (MNI) coordinates: -54, -14, -2; see Table 3.1 and Figure 3.3) when RLP was selected as a seed region. When MCI patients were compared to SCI patients, decreased connectivity in right lobule 7, 8 and right crus 2 of cerebellar hemisphere (height threshold $p < 0.001$; cluster-level FWE-corrected p = 0.003; peak (MNI) coordinates: 52, -58, -50; see Table 3.1 and Figure 3.4) were detected when PCC was selected as the seed region, and in inferior frontal and left middle frontal gyri (height threshold $p < 0.001$; cluster-level FWE-corrected p = 0.045; peak (MNI) coordinates: -50, 46, -2; see Table 3.1 and Figure 3.5) when LLP was selected as a seed region. No significant increase or decrease in functional connectivity measures were detected when MCI patients were compared to AD patients. No significant increase was detected when AD patients were compared to both MCI and SCI patients. All results were based on the WFU PickAtlas used in xjView [85], and all coordinates reported in MNI space. In Table 3.1, only significant results at a 0.001 two-sided FWE-corrected p-values were included, where Group 1 was tested against Group 2 such that $Group1 > Group2$.

Table 3.1. Clusters showing differences when Group 1 was compared to Group 2 with seed regions PCC, MPFC, LLP and RLP.

Group1	**Group2**	**Seed**	**Coordinates (x,y,z)**	$\mathbf{p}_{FWE-corr}$	**No. of voxels**
SCI	AD	PCC	24, 46, 2	0.043	118
SCI	AD	PCC	40, 8, 44	0.048	115
SCI	AD	RLP	-54, -14, -2	0.033	124
SCI	MCI	PCC	52, -58, -50	0.003	218
SCI	MCI	LLP	-50, 46, -2	0.045	127

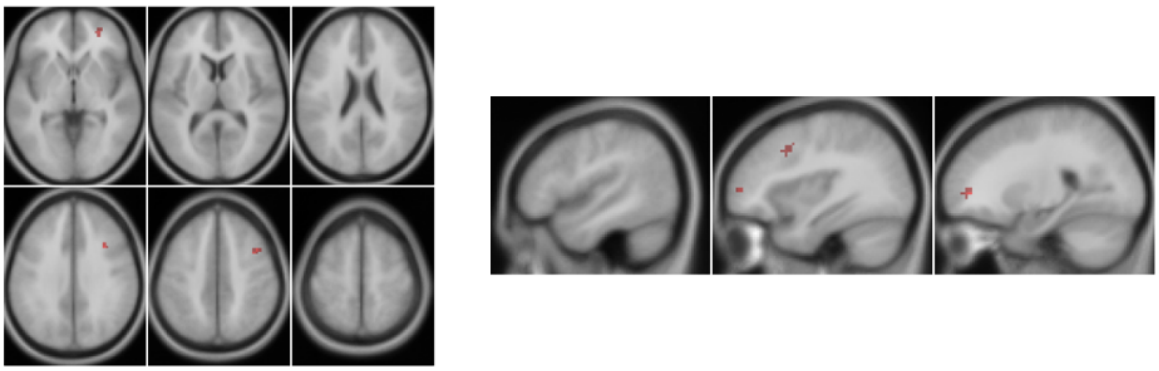

(a) (b)

Figure 3.2. When AD patients were compared to SCI patients with PCC selected as a seed region. (a) Axial View. (b) Sagittal View.

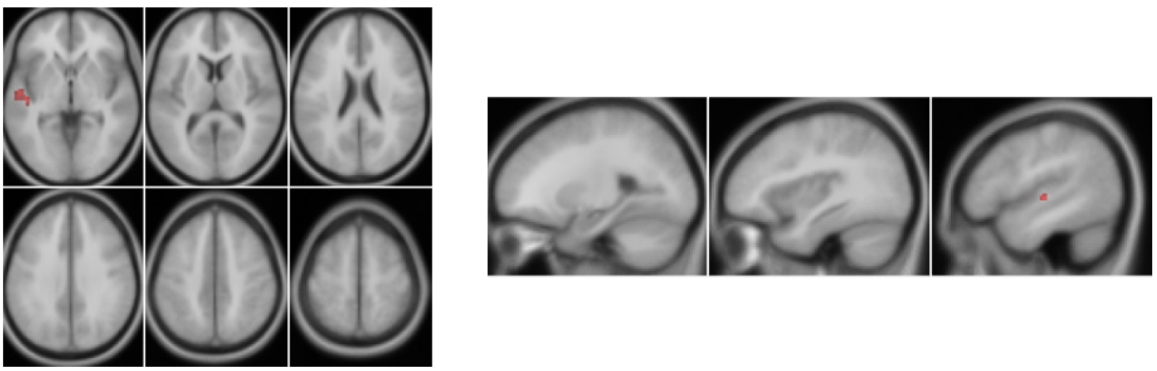

(a) (b)

Figure 3.3. When AD patients were compared to SCI patients with RLP selected as a seed region. (a) Axial View. (b) Sagittal View.

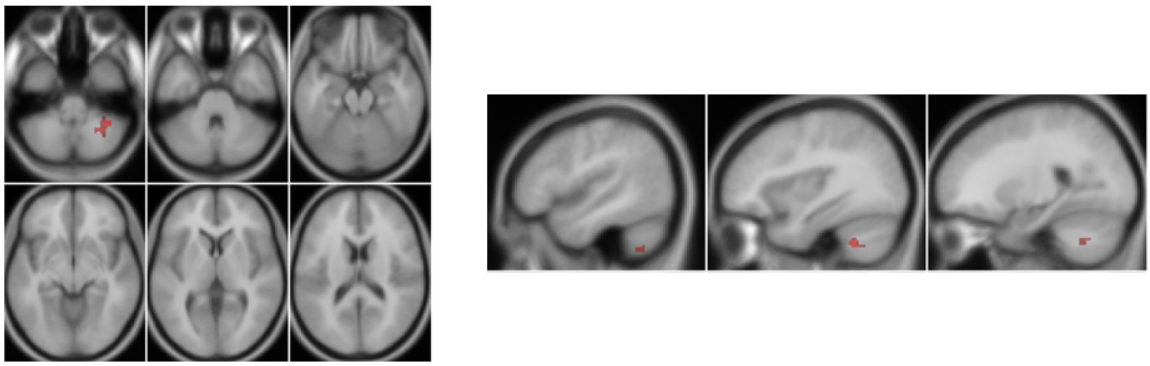

Figure 3.4. When MCI patients were compared to SCI patients with PCC selected as a seed region. (a) Axial View. (b) Sagittal View.

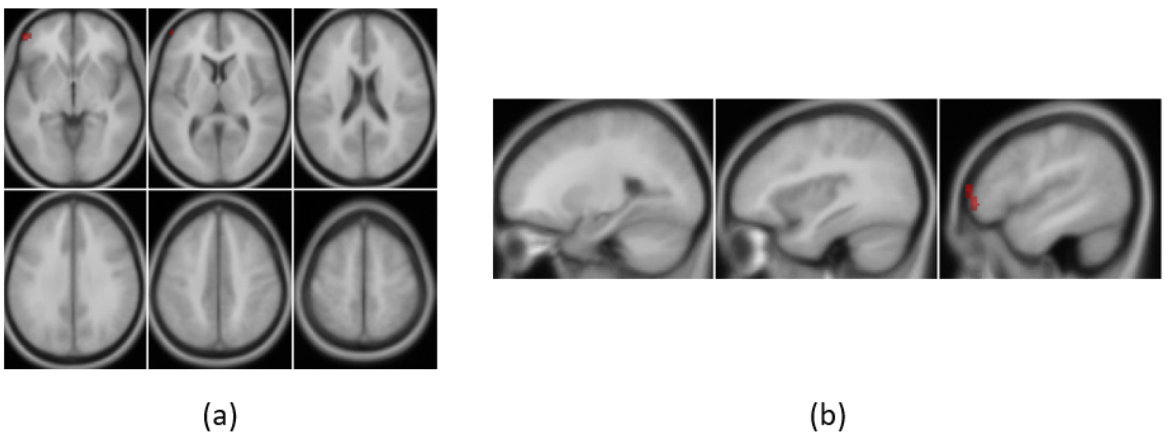

Figure 3.5. When MCI patients were compared to SCI patients with LLP selected as a seed region. (a) Axial View. (b) Sagittal View.

3.2.2. Independent Component Analysis

As an alternative to seed based analysis, group independent component analysis was conducted to analyze functional connectivity measures for the DMN components, for which Group ICA of fMRI Toolbox (GIFT) [86] was used. After spatial preprocessing, which included realignment, co-registration, normalization and smoothing

processes, the functional data went under additional pre-processing and data reduction steps, namely intensity normalization and PCA, respectively. Applying subject specific principal component analysis reduced the number of principal components to 45. The second data reduction step was applied on a group level, which reduced the number of principal components to 30. The Infomax algorithm [87] was run for 10 times in ICASSO, which was used to test the reliability of the algorithm. At the end of the ICA analysis, independent components consisting of spatial maps and associated time courses were generated.

Each independent component is composed of a spatial map and an associated time course, which are related as $\mathbf{X} = \mathbf{AS}$, where $\mathbf{X}$ is a TxV matrix, where T represents the time points and V represents the total number of voxels in the volume. The observed mixed signals are modeled as the linearly weighted sum of sources, represented by the MxV matrix $\mathbf{S}$, such as:

$$\mathbf{X}_{ij} = \sum_{k=1}^{N} \mathbf{A}_{ik}\mathbf{S}_{kj} \tag{3.4}$$

where N is number of fMRI time points. Voxel values for each component are given by the vector $\mathbf{S}_k$ ($\mathbf{S}_{kj},\ j = 1, 2, \ldots, V$, V = total number of voxels). The mixing matrix $\mathbf{A}$ gives information about how each component contributes to the observed signal [3]. In order to break signal mixtures into spatial maps and associated time courses, the inverse of the mixing matrix is used, where the unmixing matrix is $\mathbf{W} \approx \mathbf{A^{-1}}$. The unmixing matrix is used to extract source signals, $\mathbf{Y}$, from the signal mixtures, $\mathbf{X}$, as $\mathbf{Y} = \mathbf{WX}$.

When the optimality for the unmixing signal is reached, the source signals are reconstructed, $\mathbf{Y}$, which are attenuated or louder version of $\mathbf{S}$ [71]. The process requires iterative optimization of $\mathbf{W}$ for accomplishing independence among the extracted

signals, which is achieved by maximizing entropy. Entropy is used as a measure of independence, and it depends on the uniformity of a set of discrete signals, which are the extracted signals in our case.

For the group ICA analysis, infomax algorithm was used, which found independent extracted spatial sources by maximizing entropy [71, 87]. After retrieving group ICA maps, spatial-temporal regression was applied as a back reconstruction method for estimating subject specific spatial maps and corresponding time courses. Spatial-temporal regression used least squares for estimation and it was a two-step approach. The first step included estimating subject-specific time courses through spatial regression by using independent components together with the individual data in a linear model fit. The second part was the temporal regression, which used the time courses obtained from the first step to estimate subject-specific spatial maps [88].

The group independent component maps were manually inspected and the components corresponding to the Default Mode Network were selected visually by the neuroscience unit at Istanbul University, according to the network patterns described in literature. Out of 30 components, 12 were identified to be a part of a network, if not the network itself; the remaining discarded as noise or artifact sources. Among the selected components, five of them were identified as DMN related; component numbers 6 (parahippocampal), 12 (PCC), 13 (DMN posterior), 22 (small part of DMN posterior), and 29 (DMN anterior). Figures 3.6, 3.7, 3.8, 3.9 and 3.10 display individual DMN components while all the DMN related components with their relative time courses displayed at Figure 3.11.

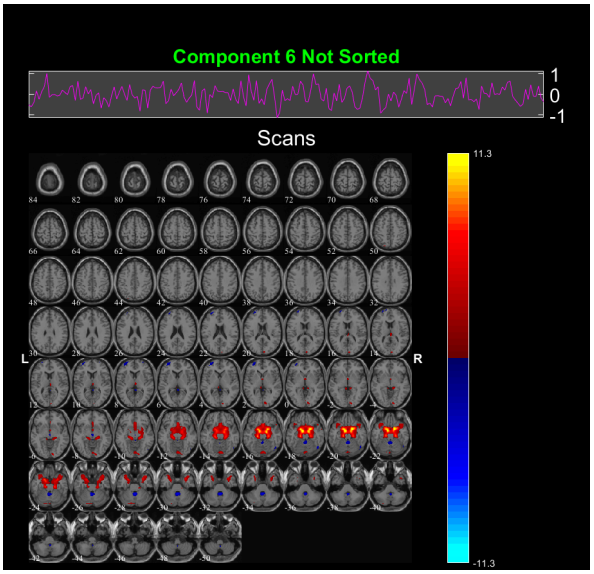

Figure 3.6. Component 6, spatial map and associated time course.

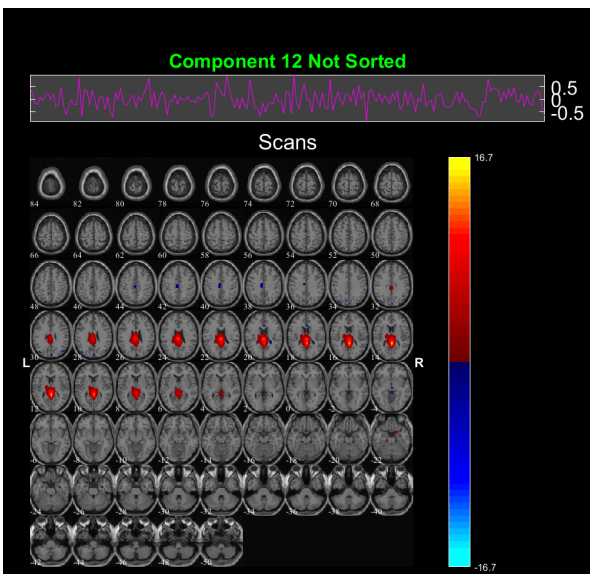

Figure 3.7. Component 12, spatial map and associated time course.

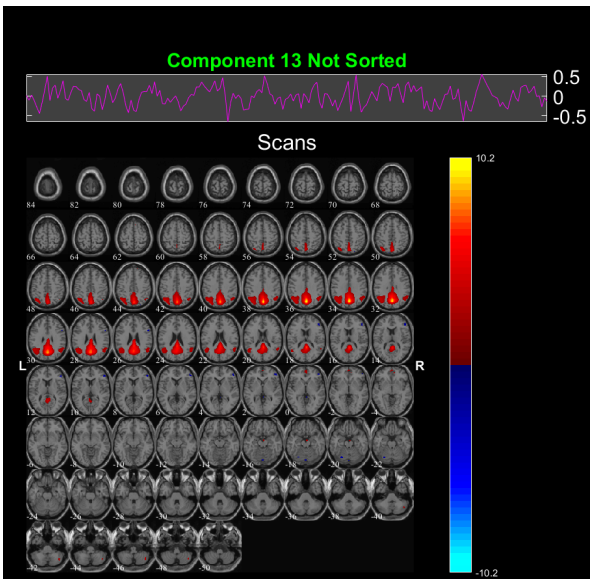

Figure 3.8. Component 13, spatial map and associated time course.

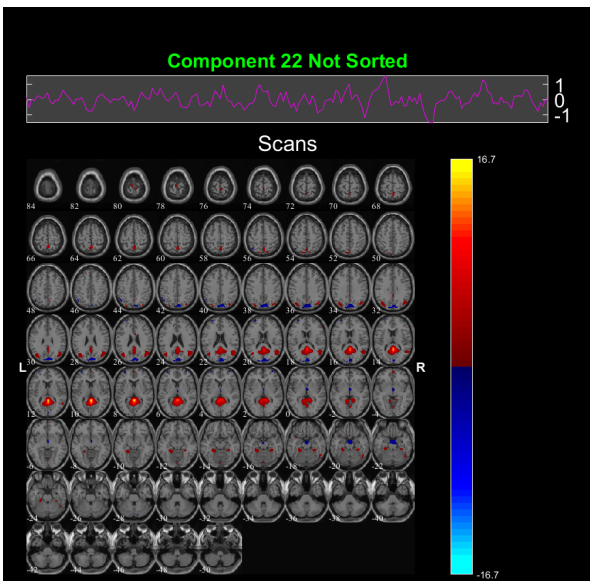

Figure 3.9. Component 22, spatial map and associated time course.

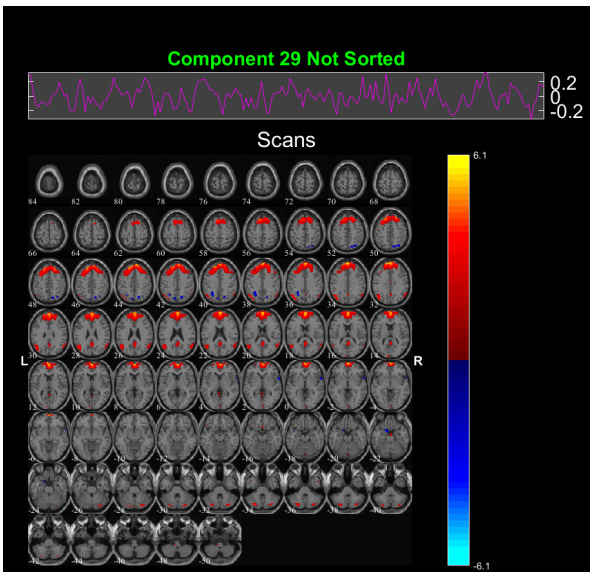

Figure 3.10. Component 29, spatial map and associated time course.

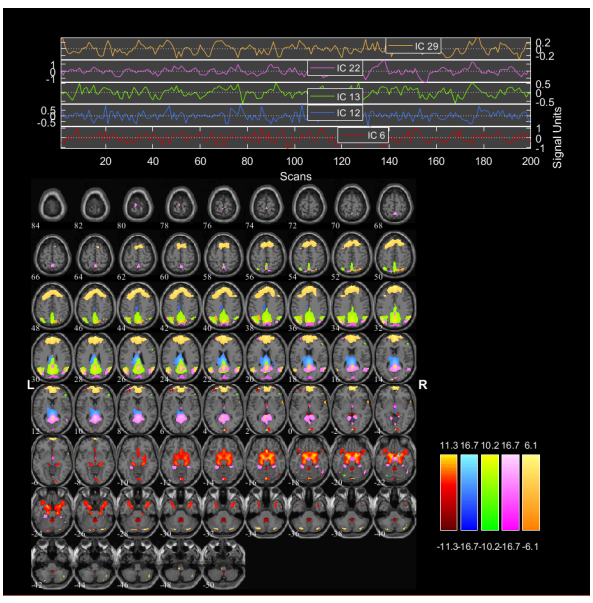

Figure 3.11. A comparison of the DMN related components, with their corresponding time courses.

Among five components used in the comparison of AD and MCI groups, AD patients showed significantly increased functional connectivity compared to MCI patients,

indicated by a significant difference for component 6. Component 6, which was previously identified as the parahippocampal area, showed greater activation in the areas parietal lobe and paracentral lobule. When AD patients were tested against the SCI patients, only one component, component 29, which was previously identified as anterior DMN, showed significant difference indicating higher functional connectivity in SCI group compared to AD patients. AD patients had decreased functional connectivity in the parahippocampal gyrus. No significant differences in functional connectivity measures were detected when MCI patients were compared to SCI patients.

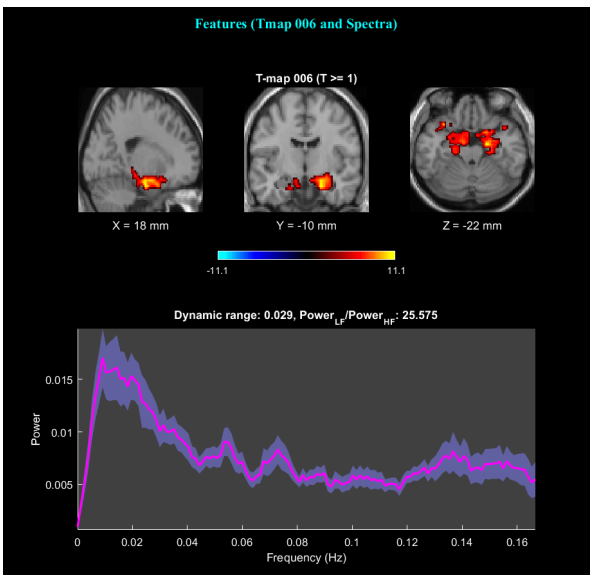

Figure 3.12. T-map for Component 6.

When cross-correlation among all components was analyzed, the highest correlation was observed between Component 6 and Component 12 as expected from the results of the statistical analyses obtained since they were representative of parahippocampal region and PCC, respectively. Fig 3.17 displays the resulting functional network connectivity correlations among components. The cross-correlation coefficients between two components were reported as z-scores. Subsequently, a cross-correlation analysis was applied to the IC time courses to test any changes in the correlation between time courses of the DMN components, shown in Fig 3.18. After applying FDR-corrected ($p < 0.05$) threshold, the correlation between component 6, parahippocampal, and component 13, posterior DMN, remained as the only significant result.

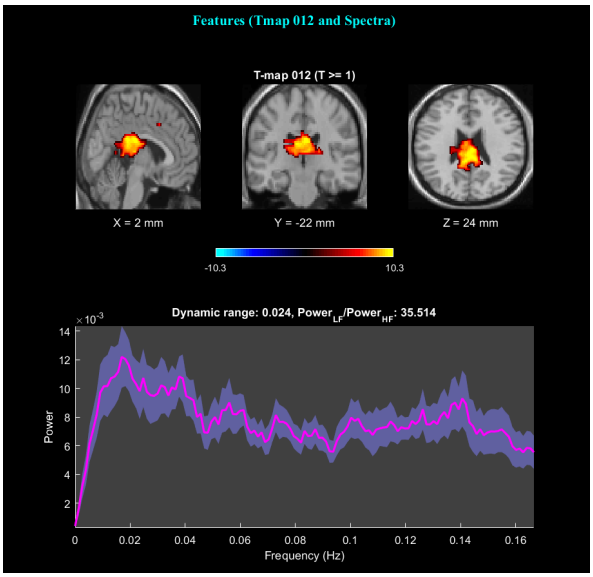

Figure 3.13. T-map for Component 12.

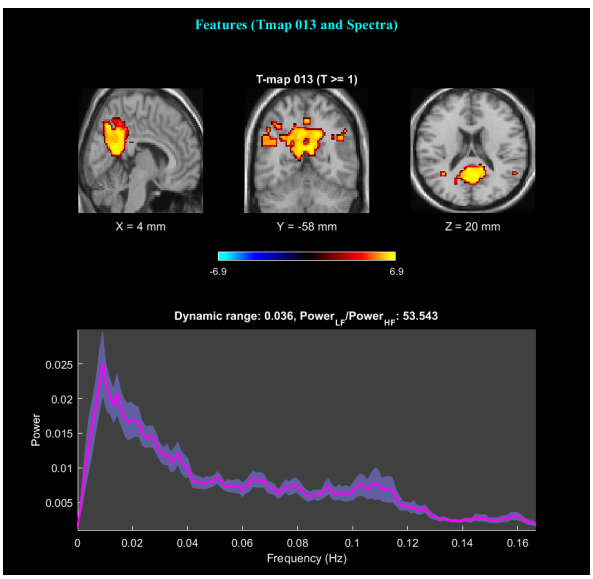

Figure 3.14. T-map for Component 13.

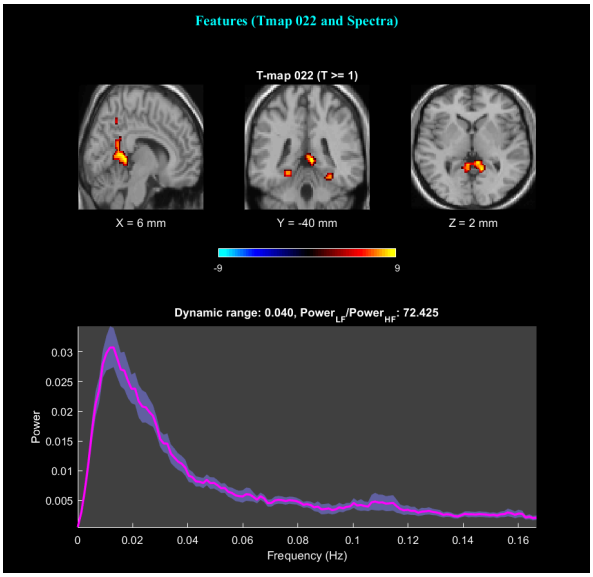

Figure 3.15. T-map for Component 22.

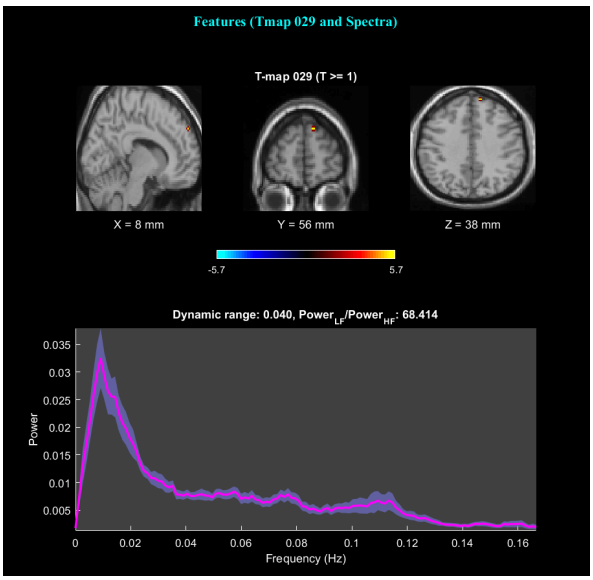

Figure 3.16. T-map for Component 29.

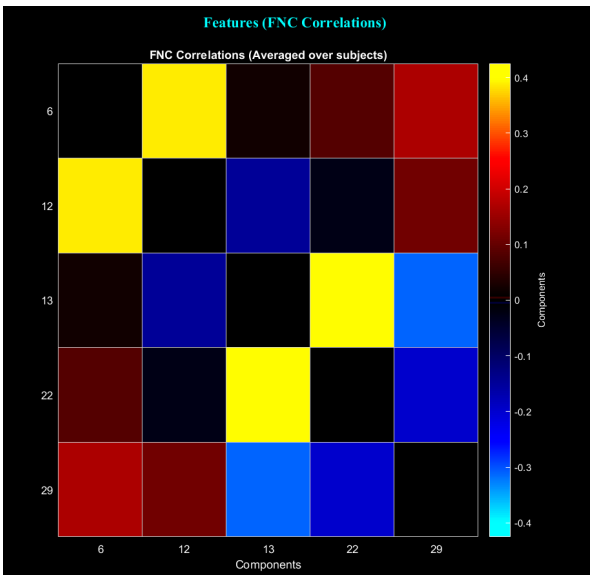

Figure 3.17. Correlations for functional network connectivity among DMN related components. Correlations were calculated using spatial maps.

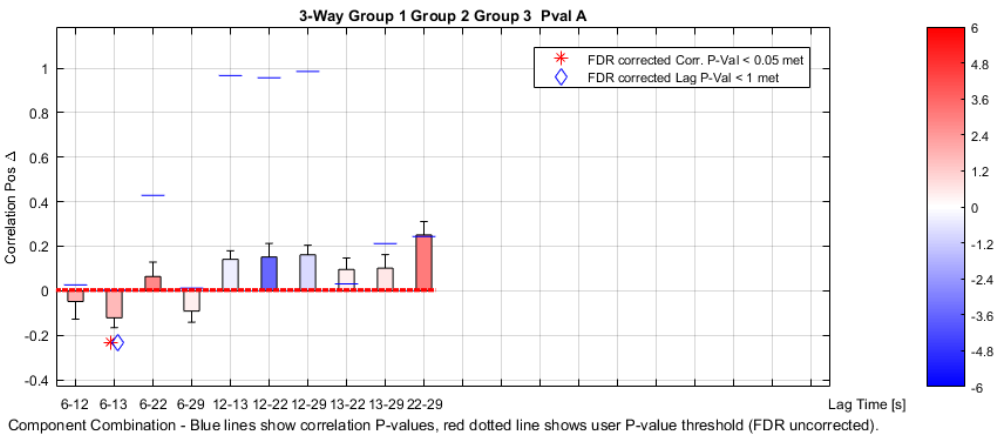

Figure 3.18. Cross-correlation of time series associated with DMN related components.

3.2.3. Cluster Analysis

For the cluster analysis, K-means clustering algorithm is selected as a method of choice. It works by assigning each data point to one of the clusters, according to a

distance measure identified by centroids [89]. K represents the number of clusters that is predefined by the user. The algorithm works in four steps: choosing an initial cluster center, computing distances from each object to the cluster center, partitioning each object to a cluster and computing the average within each cluster. The last step yields the new cluster centroid, which is iteratively used with the preceding steps until all the objects within a cluster reach the minimum distance possible [90]. Each observation is subject to the following objective functions that specify measures within-cluster, $\mathbf{I}_W$, and between-cluster, $\mathbf{I}_B$. The main objective is to minimize within-cluster, or equivalently, maximize between-cluster functions defined below [78]:

$$\mathbf{I}_W = \frac{1}{N} \sum_{k=1}^{K} \sum_{j \in \mathbf{C}_k} \mathbf{d}^2(\mathbf{z}_j, \mathbf{c}_k) \tag{3.5}$$

$$\mathbf{I}_B = \frac{1}{N} \sum_{k=1}^{K} |\mathbf{C}_k| \mathbf{d}^2(\mathbf{z}_j, \bar{\mathbf{c}}) \tag{3.6}$$

where $\mathbf{z}_j$ and $\mathbf{C}_k$ stand for voxel values and cluster centroid, respectively.

The connection measures between DMN components were selected as features for computing k-means clustering. In order to obtain the connection measures, time-series were extracted from the predefined ROIs, namely MPFC, PCC, LLP and RLP, and the zero-lag correlation coefficients were calculated between each pair. The correlation coefficients were normalized, and the obtained connectivity matrix was used for the analysis. There were two factors of interest, which have high effect on the analysis: cluster initialization and distance measure for minimization. Initially, the cluster initialization process was conducted by selecting a centroid position randomly while the second phase included seed selection by using k-means++ algorithm [91]. The

k-means++ algorithm chooses the first centroid $\mathbf{c}_1$ uniformly at random, while the second centroid, $\mathbf{c}_1$, is selected from the data set X at random with probability

$$\frac{\mathbf{d}^2(\mathbf{x}_m, \mathbf{c}_1)}{\sum_{j=1}^{n} \mathbf{d}^2(\mathbf{x}_j, \mathbf{c}_1)} \tag{3.7}$$

where the distance between the centroid and the observations is represented as $\mathbf{d}(\mathbf{x}_m, \mathbf{c}_j)$. The next step of the analysis was identifying the effect of distance measures on partitioning. Two algorithms were used for this purpose, namely Squared Euclidean and the L1 distance, defined as:

$$\mathbf{d}_{x,c} = (x - c)(x - c)' \tag{3.8}$$

and

$$\mathbf{d}_{x,c} = \sum_{j=1}^{p} |(\mathbf{x}_j - \mathbf{c}_j| \tag{3.9}$$

respectively. The algorithms were repeated for all the correlation coefficients representative of DMN within network connectivity, with number of clusters fixed at three, to compare results according to the number of groups currently available. Additionally, cluster evaluation methods were used for comparison of the number of clusters independent of the intrinsic features of the data, i.e. dementia stage. After the computations, clustering results were evaluated by using silhouette coefficients as a

measure of validation, formulated as:

$$\mathbf{S}_i = (bi - ai)/max(ai, bi) \tag{3.10}$$

where Si, ai and bi stand for the silhouette point for the ith point, the average distance within ith point and the minimum average distance between clusters from the ith point, respectively. Silhouette coefficients range between one and minus one, where each object is assigned a coefficient. Having a coefficient close to one means that the object is well-clustered, which can be interpreted as the subject is placed in a cluster correctly. The latter option, which is the negative silhouette coefficient values, indicates that the subject might be in the wrong cluster or it might be an outlier. The following Figures 3.19, 3.20, 3.21, 3.22 display the silhouette coefficients for each of the four cases:

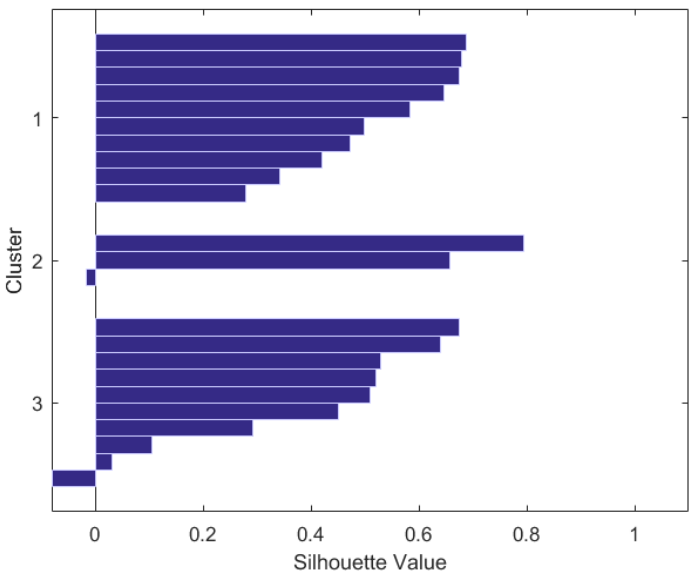

Figure 3.19. Silhouette coefficients contrast when Square Euclidean distance measure was used with random initialization.

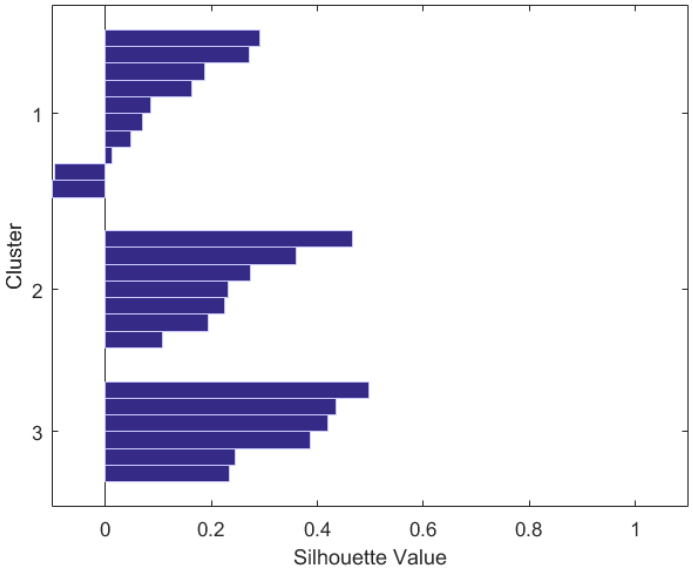

Figure 3.20. Silhouette coefficients contrast when L1 distance measure was used with random initialization.

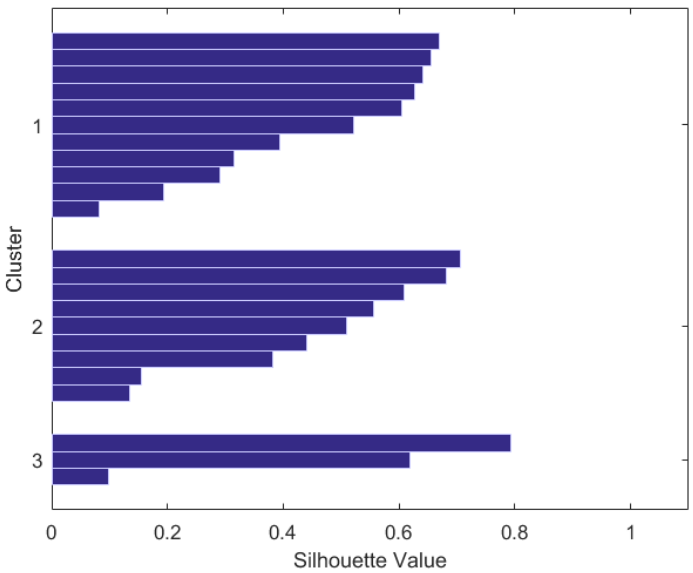

Figure 3.21. Silhouette coefficients contrast when Square Euclidean distance measure was used with k-means++ algorithm initialization.

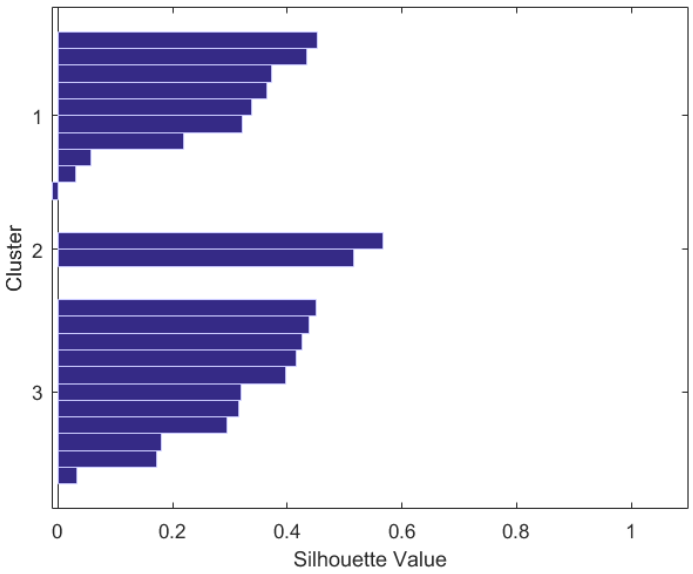

Figure 3.22. Silhouette coefficients contrast when L1 distance measure was used with k-means++ algorithm initialization.

According to the obtained results, for random cluster initialization, both Squared Euclidean and L1 methods resulted in different results. While SE outcome indicated that the subjects were clustered in groups of 10, 3 and 10; L1 resulted in clusters made of 10, 7 and 6 subjects. Both marked two subjects to be placed in wrong clusters. The results were different when the k-means++ algorithm was used for initialization. The results for both distance measures were similar; SE resulting in clusters made of 11, 9 and 3 subjects, and L1 with clusters consisting of 11, 10 and 2 subjects.

The cluster analysis was based on the fact that we have three groups of patients with 10, 8 and 5 subjects in each, namely SCI, MCI and AD, respectively, that differ from each other according to within network correlation strength. A further cluster evaluation step was applied to the data to independently test the number of clusters that can be obtained without a prior. Besides silhouette results, two more criteria were used for computing index values, namely Calinski-Harabasz and Davies-Boulding. Using Calinski-Harabasz criterion, the optimal number of clusters were determined to be two while using Davies-Boulding resulted in nine, which was the same number of

optimal clusters measured by silhouette criterion.

4. DISCUSSION AND CONCLUSION

Due to increasing amount of studies stating changes in functional connectivity measures for neurodegenerative diseases and mental illnesses, studying RSNs in depth by examining within and between connectivity measures have been a promising area of research in pursuit of a cure and possible prevention strategies involving detection of biomarkers. Dementia, as broad and complex as it is, already creates a difficult area of research due to its varying symptoms and various stages. Alzheimer's disease, being the most common form of dementia, is the focus of many studies due to its severity and, increasing number of people diagnosed with the disease. Since a cure does not exist yet, any information related to the early bio-markers of the disease is precious and in great need. Current studies indicating a relation between mild cognitive impairment and Alzheimer's disease have great importance since the relation can be used as an assessment method for early detection. Subjective cognitive impairment holds a different place as it can be used to understand possible neurological changes before any occurrence of change if the patients diagnosed with the disease can be analyzed in longitudinal studies. Default Mode Network (DMN) has a prominent space in the area of research due its intrinsic features such as having high overlaps between anatomical and functional connections, and observed change of functional connectivity between its components. This thesis is created with the main objective of investigating dementia related functional changes within the DMN, with decrease in the within network connectivity measures. Subsequently, the groups of subjects are differentiated according to their connectivity measures by using several functional connectivity analysis methods that are in frequent use. These methods fall under the general terms of seed-based and data-driven analyses, the latter including both ICA and cluster analysis.

The fMRI data used in this study was retrieved from three groups of subjects that were diagnosed with Subjective Cognitive Impairment, Mild Cognitive Impairment and Alzheimer's Disease. Prior to analyses, spatial and temporal pre-processing steps were applied on the fMRI data for removing motion related and physiological

effects. The spatial pre-processing steps included slice-timing correction, realignment, co-registering the functional data to the anatomical data, normalization and smoothing. As an additional process, the anatomical data was segmented into gray matter (GM), white matter (WM) and cerebrospinal fluid (CSF) components for further processes. After spatial pre-processing, temporal pre-processing steps were applied as a next step for further noise regression, excluding independent component analysis. For the independent component analysis (ICA), a temporal pre-processing step was omitted since ICA can successfully separate noise components and components depicting resting state networks (RSNs). Instead, a data reduction step was applied, PCA, followed by computations for algorithm stability measures. For seed-based and clustering analyses, temporal pre-processing steps included regression of WM and CSF related features and, motion regressors that are retrieved during the realignment process. For the seed-based analysis, a seed-to-voxel approach was followed, which required selection of regions-of-interest (ROI). Four regions of interests within the DMN network were selected according to their frequency of appearance in the literature. The selected regions were Posterior Cingulate Cortex (PCC), Medial Prefrontal Cortex (MPFC), Left and Right Inferior Parietal Lobe, LLP and RLP, respectively.

Initially, a seed-based approach was utilized as a method of choice for analyzing the fMRI data. The reason for selecting a seed-based analysis as an initial step was its effective and exploratory nature. Prior to conducting data-driven analysis, which comparatively outputs more complex results for interpretation, applying seed-based analysis allowed better understanding of the data. For the seed-based analysis, bivariate correlation coefficients, which were computed between seeds from DMN related areas and all other voxels, were used as a connectivity measure. Statistical analyses were applied on the resulting coefficients to draw inferences between groups. For the analyses, height threshold of $p < 0.001$ and a cluster-level extent threshold with FWE-corrected p-values, ($p < 0.05$), were selected. The results that passed the thresholds indicated that both AD and MCI patients displayed decreased functional connectivity compared to SCI group. MCI patients did not express any difference in functional connectivity measures when compared to AD patients. The areas that displayed reduced functional connectivity were detected when seeds were selected from posterior cingu-

late and lateral parietal cortices. The areas with reduced functional connectivity were majorly detected in middle and superior frontal gyri, middle and superior temporal gyri and, cerebellum crus 2 and lobule 8. Similar results were reported previously that indicate reduced functional network connectivity within prefrontal cortex, temporal lobe and cerebellum crus 2 in patients with AD compared to controls [48, 56, 92–99].

Group ICA analysis was applied for the second part of the analysis. Before the analysis, PCA and ICASSO were applied to the fMRI data for data reduction and stability testing, respectively. After ICA analysis, the independent components were visually inspected and five components that were identified as DMN related were selected for further processing. When t-test was applied, AD group showed increased activity for component 6, parahippocampal, when compared to MCI group. On the other hand, when AD group was compared to SCI group for component 29, representing anterior part of the DMN, the results indicated decreased connections in the parahippocampal gyrus. There was no significant differences when MCI group was tested against SCI, and also no increase in connectivity measures when MCI was tested against AD. The results from the cross-correlation values between the components and the time courses of the ICs also displayed changes within the DMN components including the parahippocampal area. Hence, the results obtained from the group ICA results were in line considering the analyses indicated changes of functional connectivity mainly in the parahippocampal gyrus. Similar results have been reported stating significant connectivity differences in the measurements including parahippocampal and hippocampal areas [96, 98, 100–103].

The first step for the clustering analysis included measuring ROI-to-ROI connectivity between DMN related areas, namely MPFC, PCC, LLP and RLP. For the analysis, time-series were extracted from each region of interest. Then, the zero-lag correlation coefficients were calculated between pairs of DMN ROIs, and the process was repeated for each subject. The coefficients were turned into z-scores for normalization, and the obtained 23x12 correlation coefficient matrix provided the features used for computing the k-means clustering analysis. According to the results, cluster initialization with k-means++ algorithm resulted in better results, which were similar

for both SE and L1 methods. When compared to the number of subjects included for each patient groups, k-means++ results showed alignment with number of subjects assigned to each cluster. Further analysis included cluster evaluation in order to compare different algorithms for predicting the optimal number of clusters. Two of the criteria, namely silhouette and Davies-Boulding, resulted in the same number of optimal clusters, nine. Calinski-Harabasz, on the other hand, resulted in two optimal clusters. The discrepancies about the number of subjects assigned to each cluster can be an indicative of the variability within groups that might occur due to varying stages of each condition, which was not investigated for this work.

One of the biggest challenges of resting-state fMRI analysis is that since the measures are taken without a specific frame, it is very difficult to interpret the results. This challenge is more prominent if the number of subjects is not sufficient, where sufficiency would be achieved in hundreds. Hence, it is essential and critical to use sufficient amount of subjects for the resting-state fMRI analysis. Another challenge that comes naturally with the fMRI studies is the statistical testing with accompanying correction methods. One of the biggest pitfalls of fMRI statistics is the Type 1 error, or false positives due to the number of statistical tests applied to the data for whole-brain connectivity. Nevertheless, each approach provides an invaluable insight into fMRI studies regardless of the benefits and disadvantages they have. Seed-based analysis proves to be an effective approach due to its straight-forward application and, providing easy interpretations of the results. The only major disadvantage of seed-based analysis is that the analysis is limited to the selected source seeds and their relation to other seeds. Its limitations with whole-brain analysis brings in other methods to attention, which do not proceed with selection of any seeds or regions prior to analysis. These methods, called data-driven, are very powerful approaches since they provide information without any prior assumption. However, results retrieved from data-driven approaches such as independent component analysis, cluster and graph analyses are difficult to interpret and inter-operate compared to seed-based approaches. Besides, each data-driven method introduces a difficulty associated with the method itself. Independent component analysis is an easy to apply method; however, the results are hard to explain since it requires identification of the extracted sources and separation of noise

from sources in question (via visual inspection, algorithms etc.). Similarly, clustering methods have their own characteristic properties that require some additional work compared to seed-based analysis. Specifically for the k-means algorithm, the factors such as initialization, similarity (distance) measure and number of clusters should be considered carefully since they make a great impact on the outcome. It would be more beneficial to use a seed-based approach for a detailed analysis between some regions of interests that are in question. However, for the whole-brain analysis, data-driven approaches are more preferable due to their results at whole-brain level. Additionally, the number of false positives would increase if a seed-based analysis is used for a whole-brain analysis. When investigating Default Mode Network, both seed-based and data-driven approaches are widely used in general. Default Mode Network proves to be an important network to investigate neurodegenerative diseases and their progress. This work represents results that show disrupted functional connectivity measures between sub-components of DMN when both seed-based and data-driven measures are used. Detected changes are aligned with existing work that emphasize the same subregions that are affected by the disease. The objective of future work would be centered around finding a biomarker that can differentiate between SCI, MCI and AD patient and providing an early detection mechanism. Conducting a longitudinal study with increased number of subjects would be the next step for achieving such a goal, followed by creating a framework where each data metric retrieved from different methods can be compared across subjects and conditions.

REFERENCES

1. Storti, S. F., E. Formaggio, R. Nordio, P. Manganotti, A. Fiaschi, A. Bertoldo and G. M. Toffolo, "Automatic selection of resting-state networks with functional magnetic resonance imaging", *Frontiers in neuroscience*, Vol. 7, p. 72, 2013.

2. Jack, C. R., D. S. Knopman, W. J. Jagust, R. C. Petersen, M. W. Weiner, P. S. Aisen, L. M. Shaw, P. Vemuri, H. J. Wiste, S. D. Weigand *et al.*, "Tracking pathophysiological processes in Alzheimer's disease: an updated hypothetical model of dynamic biomarkers", *The Lancet Neurology*, Vol. 12, No. 2, pp. 207–216, 2013.

3. McKeown, M. J., S. Makeig, G. G. Brown, T.-P. Jung, S. S. Kindermann, A. J. Bell and T. J. Sejnowski, *Analysis of fMRI data by blind separation into independent spatial components*, Tech. rep., DTIC Document, 1997.

4. Whitfield-Gabrieli, S. and A. Nieto-Castanon, "Conn: a functional connectivity toolbox for correlated and anticorrelated brain networks", *Brain connectivity*, Vol. 2, No. 3, pp. 125–141, 2012.

5. Huettel, S. A., A. W. Song and G. McCarthy, *Functional magnetic resonance imaging*, Vol. 1, Sinauer Associates Sunderland, 2004.

6. Smith, S. M., P. M. Matthews and P. Jezzard, *Functional MRI: an introduction to methods*, Oxford university press, 2001.

7. Friston, K., C. Frith, P. Liddle and R. Frackowiak, "Functional connectivity: the principal-component analysis of large (PET) data sets", *Journal of Cerebral Blood Flow & Metabolism*, Vol. 13, No. 1, pp. 5–14, 1993.

8. Biswal, B., F. Zerrin Yetkin, V. M. Haughton and J. S. Hyde, "Functional connectivity in the motor cortex of resting human brain using echo-planar mri", *Magnetic resonance in medicine*, Vol. 34, No. 4, pp. 537–541, 1995.

9. Raichle, M. E. and D. A. Gusnard, "Appraising the brain's energy budget", *Proceedings of the National Academy of Sciences*, Vol. 99, No. 16, pp. 10237–10239, 2002.

10. Lee, M. H., C. D. Smyser and J. S. Shimony, "Resting-state fMRI: a review of methods and clinical applications", *American Journal of Neuroradiology*, Vol. 34, No. 10, pp. 1866–1872, 2013.

11. Van Den Heuvel, M. P. and H. E. H. Pol, "Exploring the brain network: a review on resting-state fMRI functional connectivity", *European Neuropsychopharmacology*, Vol. 20, No. 8, pp. 519–534, 2010.

12. Jack, C. R., M. A. Bernstein, N. C. Fox, P. Thompson, G. Alexander, D. Harvey, B. Borowski, P. J. Britson, J. L Whitwell, C. Ward *et al.*, "The Alzheimer's disease neuroimaging initiative (ADNI): MRI methods", *Journal of Magnetic Resonance Imaging*, Vol. 27, No. 4, pp. 685–691, 2008.

13. Binnewijzend, M. A., M. M. Schoonheim, E. Sanz-Arigita, A. M. Wink, W. M. van der Flier, N. Tolboom, S. M. Adriaanse, J. S. Damoiseaux, P. Scheltens, B. N. van Berckel *et al.*, "Resting-state fMRI changes in Alzheimer's disease and mild cognitive impairment", *Neurobiology of aging*, Vol. 33, No. 9, pp. 2018–2028, 2012.

14. Garcia-Ptacek, S., L. Cavallin, I. Kåreholt, M. G. Kramberger, B. Winblad, V. Jelic and M. Eriksdotter, "Subjective cognitive impairment subjects in our clinical practice", *Dementia and geriatric cognitive disorders extra*, Vol. 4, No. 3, pp. 419–430, 2014.

15. Damoiseaux, J. S., K. E. Prater, B. L. Miller and M. D. Greicius, "Functional connectivity tracks clinical deterioration in Alzheimer's disease", *Neurobiology of aging*, Vol. 33, No. 4, pp. 828–e19, 2012.

16. Liang, P., Z. Wang, Y. Yang, X. Jia and K. Li, "Functional disconnection and

compensation in mild cognitive impairment: evidence from DLPFC connectivity using resting-state fMRI", *PloS one*, Vol. 6, No. 7, p. e22153, 2011.

17. Van Den Heuvel, M. P., R. C. Mandl, R. S. Kahn, H. Pol and E. Hilleke, "Functionally linked resting-state networks reflect the underlying structural connectivity architecture of the human brain", *Human brain mapping*, Vol. 30, No. 10, pp. 3127–3141, 2009.

18. Wu, L., T. Eichele and V. D. Calhoun, "Reactivity of hemodynamic responses and functional connectivity to different states of alpha synchrony: a concurrent EEG-fMRI study", *Neuroimage*, Vol. 52, No. 4, pp. 1252–1260, 2010.

19. Benjamin, C., D. A. Lieberman, M. Chang, N. Ofen, S. Whitfield-Gabrieli, J. D. Gabrieli and N. Gaab, "The influence of rest period instructions on the default mode network", *Frontiers in human neuroscience*, Vol. 4, p. 218, 2010.

20. Smith, S. M., K. L. Miller, G. Salimi-Khorshidi, M. Webster, C. F. Beckmann, T. E. Nichols, J. D. Ramsey and M. W. Woolrich, "Network modelling methods for FMRI", *Neuroimage*, Vol. 54, No. 2, pp. 875–891, 2011.

21. Beckmann, C. F., M. DeLuca, J. T. Devlin and S. M. Smith, "Investigations into resting-state connectivity using independent component analysis", *Philosophical Transactions of the Royal Society of London B: Biological Sciences*, Vol. 360, No. 1457, pp. 1001–1013, 2005.

22. Damoiseaux, J., S. Rombouts, F. Barkhof, P. Scheltens, C. Stam, S. M. Smith and C. Beckmann, "Consistent resting-state networks across healthy subjects", *Proceedings of the national academy of sciences*, Vol. 103, No. 37, pp. 13848–13853, 2006.

23. Damoiseaux, J., C. Beckmann, E. S. Arigita, F. Barkhof, P. Scheltens, C. Stam, S. Smith and S. Rombouts, "Reduced resting-state brain activity in the "default network" in normal aging", *Cerebral cortex*, Vol. 18, No. 8, pp. 1856–1864, 2008.

24. Horn, A., D. Ostwald, M. Reisert and F. Blankenburg, "The structural–functional connectome and the default mode network of the human brain", *Neuroimage*, Vol. 102, pp. 142–151, 2014.

25. Tao, Y., B. Liu, X. Zhang, J. Li, W. Qin, C. Yu and T. Jiang, "The Structural Connectivity Pattern of the Default Mode Network and Its Association with Memory and Anxiety", *Frontiers in neuroanatomy*, Vol. 9, 2015.

26. Raichle, M. E., A. M. MacLeod, A. Z. Snyder, W. J. Powers, D. A. Gusnard and G. L. Shulman, "A default mode of brain function", *Proceedings of the National Academy of Sciences*, Vol. 98, No. 2, pp. 676–682, 2001.

27. Gusnard, D. A. and M. E. Raichle, "Searching for a baseline: functional imaging and the resting human brain", *Nature Reviews Neuroscience*, Vol. 2, No. 10, pp. 685–694, 2001.

28. Greicius, M. D., B. Krasnow, A. L. Reiss and V. Menon, "Functional connectivity in the resting brain: a network analysis of the default mode hypothesis", *Proceedings of the National Academy of Sciences*, Vol. 100, No. 1, pp. 253–258, 2003.

29. Satterthwaite, T. D., M. A. Elliott, R. T. Gerraty, K. Ruparel, J. Loughead, M. E. Calkins, S. B. Eickhoff, H. Hakonarson, R. C. Gur, R. E. Gur *et al.*, "An improved framework for confound regression and filtering for control of motion artifact in the preprocessing of resting-state functional connectivity data", *Neuroimage*, Vol. 64, pp. 240–256, 2013.

30. Allen, E. A., E. Damaraju, S. M. Plis, E. B. Erhardt, T. Eichele and V. D. Calhoun, "Tracking whole-brain connectivity dynamics in the resting state", *Cerebral cortex*, p. bhs352, 2012.

31. Simic, G., M. Babic, F. Borovecki and P. R. Hof, "Early Failure of the Default-Mode Network and the Pathogenesis of Alzheimer's Disease", *CNS neuroscience*

& therapeutics, Vol. 20, No. 7, pp. 692–698, 2014.

32. Hampel, H., K. Bürger, S. J. Teipel, A. L. Bokde, H. Zetterberg and K. Blennow, "Core candidate neurochemical and imaging biomarkers of Alzheimer's disease", *Alzheimer's & Dementia*, Vol. 4, No. 1, pp. 38–48, 2008.

33. Sheline, Y. I., M. E. Raichle, A. Z. Snyder, J. C. Morris, D. Head, S. Wang and M. A. Mintun, "Amyloid plaques disrupt resting state default mode network connectivity in cognitively normal elderly", *Biological psychiatry*, Vol. 67, No. 6, pp. 584–587, 2010.

34. Seeley, W. W., R. K. Crawford, J. Zhou, B. L. Miller and M. D. Greicius, "Neurodegenerative diseases target large-scale human brain networks", *Neuron*, Vol. 62, No. 1, pp. 42–52, 2009.

35. Whitfield-Gabrieli, S., H. W. Thermenos, S. Milanovic, M. T. Tsuang, S. V. Faraone, R. W. McCarley, M. E. Shenton, A. I. Green, A. Nieto-Castanon, P. LaViolette *et al.*, "Hyperactivity and hyperconnectivity of the default network in schizophrenia and in first-degree relatives of persons with schizophrenia", *Proceedings of the National Academy of Sciences*, Vol. 106, No. 4, pp. 1279–1284, 2009.

36. Garrity, A. G., G. D. Pearlson, K. McKiernan, D. Lloyd, K. A. Kiehl and V. D. Calhoun, "Aberrant "default mode" functional connectivity in schizophrenia", *American journal of psychiatry*, Vol. 164, No. 3, pp. 450–457, 2007.

37. Haslinger, B., P. Erhard, N. Kämpfe, H. Boecker, E. Rummeny, M. Schwaiger, B. Conrad and A. Ceballos-Baumann, "Event-related functional magnetic resonance imaging in Parkinson's disease before and after levodopa", *Brain*, Vol. 124, No. 3, pp. 558–570, 2001.

38. Vo, A., W. Sako, K. Fujita, S. Peng, P. J. Mattis, F. M. Skidmore, Y. Ma, A. M. Uluğ and D. Eidelberg, "Parkinson's disease-related network topographies

characterized with resting state functional MRI", *Human brain mapping*, 2016.

39. Hou, Y., J. Yang, C. Luo, W. Song, R. Ou, W. Liu, Q. Gong and H. Shang, "Dysfunction of the Default Mode Network in Drug-Naïve Parkinson's Disease with Mild Cognitive Impairments: A Resting-State fMRI Study", *Frontiers in aging neuroscience*, Vol. 8, 2016.

40. Sheline, Y. I., D. M. Barch, J. M. Donnelly, J. M. Ollinger, A. Z. Snyder and M. A. Mintun, "Increased amygdala response to masked emotional faces in depressed subjects resolves with antidepressant treatment: an fMRI study", *Biological psychiatry*, Vol. 50, No. 9, pp. 651–658, 2001.

41. Veer, I. M., C. Beckmann, M.-J. Van Tol, L. Ferrarini, J. Milles, D. Veltman, A. Aleman, M. A. Van Buchem, N. J. Van Der Wee and S. A. Rombouts, "Whole brain resting-state analysis reveals decreased functional connectivity in major depression", *Frontiers in systems neuroscience*, Vol. 4, p. 41, 2010.

42. Murrough, J. W., C. G. Abdallah, A. Anticevic, K. A. Collins, P. Geha, L. A. Averill, J. Schwartz, K. E. DeWilde, C. Averill, G. Jia-Wei Yang *et al.*, "Reduced global functional connectivity of the medial prefrontal cortex in major depressive disorder", *Human brain mapping*, Vol. 37, No. 43, pp. 3214–3223, 2016.

43. Witiuk, K., J. Fernandez-Ruiz, R. McKee, N. Alahyane, B. C. Coe, M. Melanson and D. P. Munoz, "Cognitive deterioration and functional compensation in ALS measured with fMRI using an inhibitory task", *The Journal of Neuroscience*, Vol. 34, No. 43, pp. 14260–14271, 2014.

44. Ferreira, L. K. and G. F. Busatto, "Resting-state functional connectivity in normal brain aging", *Neuroscience & Biobehavioral Reviews*, Vol. 37, No. 3, pp. 384–400, 2013.

45. Mevel, K., B. Landeau, M. Fouquet, R. La Joie, N. Villain, F. Mézenge, A. Perrotin, F. Eustache, B. Desgranges and G. Chételat, "Age effect on the default

mode network, inner thoughts, and cognitive abilities", *Neurobiology of aging*, Vol. 34, No. 4, pp. 1292–1301, 2013.

46. Hedden, T., K. R. Van Dijk, J. A. Becker, A. Mehta, R. A. Sperling, K. A. Johnson and R. L. Buckner, "Disruption of functional connectivity in clinically normal older adults harboring amyloid burden", *The Journal of neuroscience*, Vol. 29, No. 40, pp. 12686–12694, 2009.

47. Hafkemeijer, A., I. Altmann-Schneider, A. M. Oleksik, L. van de Wiel, H. A. Middelkoop, M. A. van Buchem, J. van der Grond and S. A. Rombouts, "Increased functional connectivity and brain atrophy in elderly with subjective memory complaints", *Brain connectivity*, Vol. 3, No. 4, pp. 353–362, 2013.

48. Sheline, Y. I. and M. E. Raichle, "Resting state functional connectivity in preclinical Alzheimer's disease", *Biological psychiatry*, Vol. 74, No. 5, pp. 340–347, 2013.

49. Brier, M. R., J. B. Thomas, A. Z. Snyder, T. L. Benzinger, D. Zhang, M. E. Raichle, D. M. Holtzman, J. C. Morris and B. M. Ances, "Loss of intranetwork and internetwork resting state functional connections with Alzheimer's disease progression", *The Journal of neuroscience*, Vol. 32, No. 26, pp. 8890–8899, 2012.

50. Zhou, J., M. D. Greicius, E. D. Gennatas, M. E. Growdon, J. Y. Jang, G. D. Rabinovici, J. H. Kramer, M. Weiner, B. L. Miller and W. W. Seeley, "Divergent network connectivity changes in behavioural variant frontotemporal dementia and Alzheimer's disease", *Brain*, Vol. 133, No. 5, pp. 1352–1367, 2010.

51. Gauthier, S., B. Reisberg, M. Zaudig, R. C. Petersen, K. Ritchie, K. Broich, S. Belleville, H. Brodaty, D. Bennett, H. Chertkow *et al.*, "Mild cognitive impairment", *The Lancet*, Vol. 367, No. 9518, pp. 1262–1270, 2006.

52. Wee, C.-Y., P.-T. Yap, D. Zhang, K. Denny, J. N. Browndyke, G. G. Potter, K. A. Welsh-Bohmer, L. Wang and D. Shen, "Identification of MCI individuals using

structural and functional connectivity networks", *Neuroimage*, Vol. 59, No. 3, pp. 2045–2056, 2012.

53. Bai, F., Z. Zhang, H. Yu, Y. Shi, Y. Yuan, W. Zhu, X. Zhang and Y. Qian, "Default-mode network activity distinguishes amnestic type mild cognitive impairment from healthy aging: a combined structural and resting-state functional MRI study", *Neuroscience letters*, Vol. 438, No. 1, pp. 111–115, 2008.

54. McKenna, F., B.-B. Koo, R. Killiany, A. D. N. Initiative *et al.*, "Comparison of ApoE-related brain connectivity differences in early MCI and normal aging populations: an fMRI study", *Brain imaging and behavior*, pp. 1–14, 2015.

55. Grundman, M., R. C. Petersen, S. H. Ferris, R. G. Thomas, P. S. Aisen, D. A. Bennett, N. L. Foster, C. R. Jack Jr, D. R. Galasko, R. Doody *et al.*, "Mild cognitive impairment can be distinguished from Alzheimer disease and normal aging for clinical trials", *Archives of neurology*, Vol. 61, No. 1, pp. 59–66, 2004.

56. Damoiseaux, J. S., "Resting-state fMRI as a biomarker for Alzheimer's disease?", *Alzheimer's research & therapy*, Vol. 4, No. 2, p. 1, 2012.

57. Mistur, R., L. Mosconi, S. D. Santi, M. Guzman, Y. Li, W. Tsui and M. J. de Leon, "Current challenges for the early detection of Alzheimer's disease: brain imaging and CSF studies", *Journal of Clinical Neurology*, Vol. 5, No. 4, pp. 153–166, 2009.

58. Li, S.-J., Z. Li, G. Wu, M.-J. Zhang, M. Franczak and P. G. Antuono, "Alzheimer disease: evaluation of a functional mr imaging index as a marker 1", *Radiology*, Vol. 225, No. 1, pp. 253–259, 2002.

59. Craig-Schapiro, R., A. M. Fagan and D. M. Holtzman, "Biomarkers of Alzheimer's disease", *Neurobiology of disease*, Vol. 35, No. 2, pp. 128–140, 2009.

60. Counts, S. E., M. D. Ikonomovic, N. Mercado, I. E. Vega and E. J. Mufson, "Biomarkers for the Early Detection and Progression of Alzheimer's Disease",

Neurotherapeutics, pp. 1–19, 2016.

61. Harrison, T. M., A. C. Burggren, G. W. Small and S. Y. Bookheimer, "Altered memory-related functional connectivity of the anterior and posterior hippocampus in older adults at increased genetic risk for Alzheimer's disease", *Human brain mapping*, Vol. 37, No. 1, pp. 366–380, 2016.

62. Zhou, Y., C. Tan, D. Wen, H. Sun, W. Han and Y. Xu, "The Biomarkers for Identifying Preclinical Alzheimer's Disease via Structural and Functional Magnetic Resonance Imaging", *Frontiers in aging neuroscience*, Vol. 8, 2016.

63. Allen, G., H. Barnard, R. McColl, A. L. Hester, J. A. Fields, M. F. Weiner, W. K. Ringe, A. M. Lipton, M. Brooker, E. McDonald *et al.*, "Reduced hippocampal functional connectivity in Alzheimer disease", *Archives of neurology*, Vol. 64, No. 10, pp. 1482–1487, 2007.

64. Honey, C., O. Sporns, L. Cammoun, X. Gigandet, J.-P. Thiran, R. Meuli and P. Hagmann, "Predicting human resting-state functional connectivity from structural connectivity", *Proceedings of the National Academy of Sciences*, Vol. 106, No. 6, pp. 2035–2040, 2009.

65. Dipasquale, O., L. Griffanti, M. Clerici, R. Nemni, G. Baselli and F. Baglio, "High-dimensional ICA analysis detects within-network functional connectivity damage of default-mode and sensory-motor networks in Alzheimer's disease", *Frontiers in human neuroscience*, Vol. 9, p. 43, 2015.

66. Greicius, M. D., G. Srivastava, A. L. Reiss and V. Menon, "Default-mode network activity distinguishes Alzheimer's disease from healthy aging: evidence from functional MRI", *Proceedings of the National Academy of Sciences of the United States of America*, Vol. 101, No. 13, pp. 4637–4642, 2004.

67. Lehmann, M., C. Madison, P. M. Ghosh, Z. A. Miller, M. D. Greicius, J. H. Kramer, G. Coppola, B. L. Miller, W. J. Jagust, M. L. Gorno-Tempini *et al.*, "Loss

of functional connectivity is greater outside the default mode network in nonfamilial early-onset Alzheimer's disease variants", *Neurobiology of aging*, Vol. 36, No. 10, pp. 2678–2686, 2015.

68. Bai, F., D. R. Watson, H. Yu, Y. Shi, Y. Yuan and Z. Zhang, "Abnormal resting-state functional connectivity of posterior cingulate cortex in amnestic type mild cognitive impairment", *Brain research*, Vol. 1302, pp. 167–174, 2009.

69. Gardini, S., A. Venneri, F. Sambataro, F. Cuetos, F. Fasano, M. Marchi, G. Crisi and P. Caffarra, "Increased functional connectivity in the default mode network in mild cognitive impairment: a maladaptive compensatory mechanism associated with poor semantic memory performance", *Journal of Alzheimer's Disease*, Vol. 45, No. 2, pp. 457–470, 2015.

70. Power, J. D., A. Mitra, T. O. Laumann, A. Z. Snyder, B. L. Schlaggar and S. E. Petersen, "Methods to detect, characterize, and remove motion artifact in resting state fMRI", *Neuroimage*, Vol. 84, pp. 320–341, 2014.

71. Stone, J. V., *Independent component analysis*, Wiley Online Library, 2004.

72. Poldrack, R. A., "Region of interest analysis for fMRI", *Social cognitive and affective neuroscience*, Vol. 2, No. 1, pp. 67–70, 2007.

73. Hyvärinen, A. and E. Oja, "Independent component analysis: algorithms and applications", *Neural networks*, Vol. 13, No. 4, pp. 411–430, 2000.

74. Calhoun, V., T. Adali, G. Pearlson and J. Pekar, "A method for making group inferences from functional MRI data using independent component analysis", *Human brain mapping*, Vol. 14, No. 3, pp. 140–151, 2001.

75. Calhoun, V. D., T. Eichele, T. Adalı and E. A. Allen, "Decomposing the brain: components and modes, networks and nodes", *Trends in cognitive sciences*, Vol. 16, No. 5, pp. 255–256, 2012.

76. Venkataraman, A., K. R. Van Dijk, R. L. Buckner and P. Golland, "Exploring functional connectivity in fMRI via clustering", *2009 IEEE International Conference on Acoustics, Speech and Signal Processing*, pp. 441–444, IEEE, 2009.

77. Wu, E. H. and L. Philip, "Independent component analysis for clustering multivariate time series data", *International Conference on Advanced Data Mining and Applications*, pp. 474–482, Springer, 2005.

78. Goutte, C., P. Toft, E. Rostrup, F. Å. Nielsen and L. K. Hansen, "On clustering fMRI time series", *NeuroImage*, Vol. 9, No. 3, pp. 298–310, 1999.

79. Heller, R., D. Stanley, D. Yekutieli, N. Rubin and Y. Benjamini, "Cluster-based analysis of FMRI data", *NeuroImage*, Vol. 33, No. 2, pp. 599–608, 2006.

80. "SPM12", `http://www.fil.ion.ucl.ac.uk/spm/`, 2017, accessed at December 2016.

81. "CONN Toolbox", `http://www.nitrc.org/projects/conn`, 2017, accessed at December 2016.

82. Behzadi, Y., K. Restom, J. Liau and T. T. Liu, "A component based noise correction method (CompCor) for BOLD and perfusion based fMRI", *Neuroimage*, Vol. 37, No. 1, pp. 90–101, 2007.

83. Worsley, K. J., C. Liao, J. Aston, V. Petre, G. Duncan, F. Morales and A. Evans, "A general statistical analysis for fMRI data", *Neuroimage*, Vol. 15, No. 1, pp. 1–15, 2002.

84. Buckner, R. L., J. Sepulcre, T. Talukdar, F. M. Krienen, H. Liu, T. Hedden, J. R. Andrews-Hanna, R. A. Sperling and K. A. Johnson, "Cortical hubs revealed by intrinsic functional connectivity: mapping, assessment of stability, and relation to Alzheimer's disease", *The Journal of Neuroscience*, Vol. 29, No. 6, pp. 1860–1873, 2009.

85. Cui, X., J. Li and X. Song, "xjView", `http://www.alivelearn.net/xjview/`, 2017.

86. "GIFT", `http://mialab.mrn.org/software/gift/index.html`, 2017, accessed at December 2016.

87. Bell, A. J. and T. J. Sejnowski, "An information-maximization approach to blind separation and blind deconvolution", *Neural computation*, Vol. 7, No. 6, pp. 1129–1159, 1995.

88. Erhardt, E. B., S. Rachakonda, E. J. Bedrick, E. A. Allen, T. Adali and V. D. Calhoun, "Comparison of multi-subject ICA methods for analysis of fMRI data", *Human brain mapping*, Vol. 32, No. 12, pp. 2075–2095, 2011.

89. Lloyd, S., "Least squares quantization in PCM", *IEEE transactions on information theory*, Vol. 28, No. 2, pp. 129–137, 1982.

90. Liao, T. W., "Clustering of time series data—a survey", *Pattern recognition*, Vol. 38, No. 11, pp. 1857–1874, 2005.

91. Arthur, D. and S. Vassilvitskii, "k-means++: The advantages of careful seeding", *Proceedings of the eighteenth annual ACM-SIAM symposium on Discrete algorithms*, pp. 1027–1035, Society for Industrial and Applied Mathematics, 2007.

92. Zhang, H.-Y., S.-J. Wang, J. Xing, B. Liu, Z.-L. Ma, M. Yang, Z.-J. Zhang and G.-J. Teng, "Detection of PCC functional connectivity characteristics in resting-state fMRI in mild Alzheimer's disease", *Behavioural brain research*, Vol. 197, No. 1, pp. 103–108, 2009.

93. Wang, K., M. Liang, L. Wang, L. Tian, X. Zhang, K. Li and T. Jiang, "Altered functional connectivity in early Alzheimer's disease: a resting-state fMRI study", *Human brain mapping*, Vol. 28, No. 10, pp. 967–978, 2007.

94. He, Y., L. Wang, Y. Zang, L. Tian, X. Zhang, K. Li and T. Jiang, "Regional coherence changes in the early stages of Alzheimer's disease: a combined structural and resting-state functional MRI study", *Neuroimage*, Vol. 35, No. 2, pp. 488–500, 2007.

95. Zhang, H.-Y., S.-J. Wang, B. Liu, Z.-L. Ma, M. Yang, Z.-J. Zhang and G.-J. Teng, "Resting Brain Connectivity: Changes during the Progress of Alzheimer Disease 1", *Radiology*, Vol. 256, No. 2, pp. 598–606, 2010.

96. Celone, K. A., V. D. Calhoun, B. C. Dickerson, A. Atri, E. F. Chua, S. L. Miller, K. DePeau, D. M. Rentz, D. J. Selkoe, D. Blacker *et al.*, "Alterations in memory networks in mild cognitive impairment and Alzheimer's disease: an independent component analysis", *The Journal of neuroscience*, Vol. 26, No. 40, pp. 10222–10231, 2006.

97. Sheline, Y. I., J. C. Morris, A. Z. Snyder, J. L. Price, Z. Yan, G. D'Angelo, C. Liu, S. Dixit, T. Benzinger, A. Fagan *et al.*, "APOE4 allele disrupts resting state fMRI connectivity in the absence of amyloid plaques or decreased CSF Aβ42", *The Journal of Neuroscience*, Vol. 30, No. 50, pp. 17035–17040, 2010.

98. Filippini, N., B. J. MacIntosh, M. G. Hough, G. M. Goodwin, G. B. Frisoni, S. M. Smith, P. M. Matthews, C. F. Beckmann and C. E. Mackay, "Distinct patterns of brain activity in young carriers of the APOE-ε4 allele", *Proceedings of the National Academy of Sciences*, Vol. 106, No. 17, pp. 7209–7214, 2009.

99. Sang, L., W. Qin, Y. Liu, W. Han, Y. Zhang, T. Jiang and C. Yu, "Resting-state functional connectivity of the vermal and hemispheric subregions of the cerebellum with both the cerebral cortical networks and subcortical structures", *Neuroimage*, Vol. 61, No. 4, pp. 1213–1225, 2012.

100. Ward, A. M., A. P. Schultz, W. Huijbers, K. R. Dijk, T. Hedden and R. A. Sperling, "The parahippocampal gyrus links the default-mode cortical network with the medial temporal lobe memory system", *Human brain mapping*, Vol. 35,

No. 3, pp. 1061–1073, 2014.

101. Wang, L., Y. Zang, Y. He, M. Liang, X. Zhang, L. Tian, T. Wu, T. Jiang and K. Li, "Changes in hippocampal connectivity in the early stages of Alzheimer's disease: evidence from resting state fMRI", *Neuroimage*, Vol. 31, No. 2, pp. 496–504, 2006.

102. Cai, S., T. Chong, Y. Zhang, J. Li, K. M. von Deneen, J. Ren, M. Dong, L. Huang, A. D. N. Initiative *et al.*, "Altered functional connectivity of fusiform gyrus in subjects with amnestic mild cognitive impairment: a resting-state fMRI study", *Frontiers in human neuroscience*, Vol. 9, 2015.

103. Westlye, E. T., A. Lundervold, H. Rootwelt, A. J. Lundervold and L. T. Westlye, "Increased hippocampal default mode synchronization during rest in middle-aged and elderly APOE $\varepsilon 4$ carriers: relationships with memory performance", *The Journal of Neuroscience*, Vol. 31, No. 21, pp. 7775–7783, 2011.

APPENDIX A: APPLICATION

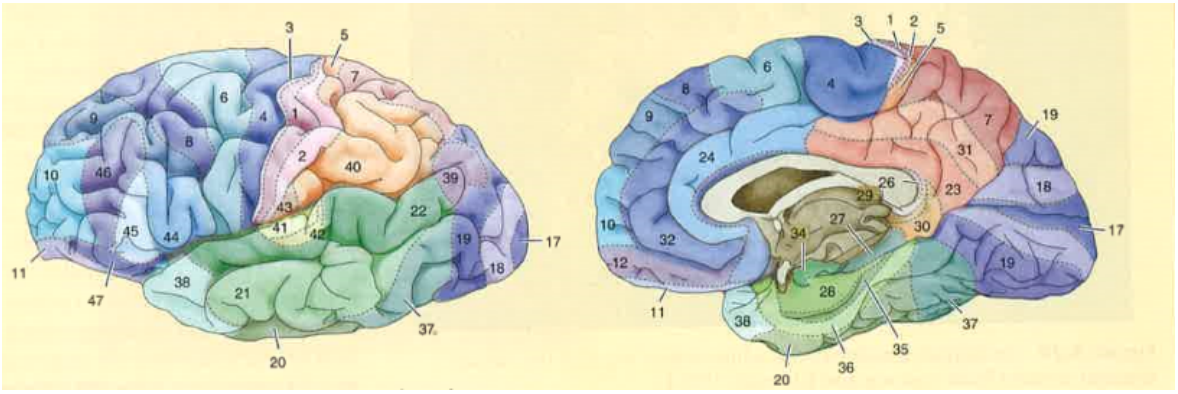

Figure A.1. Map of Broadmann [5].

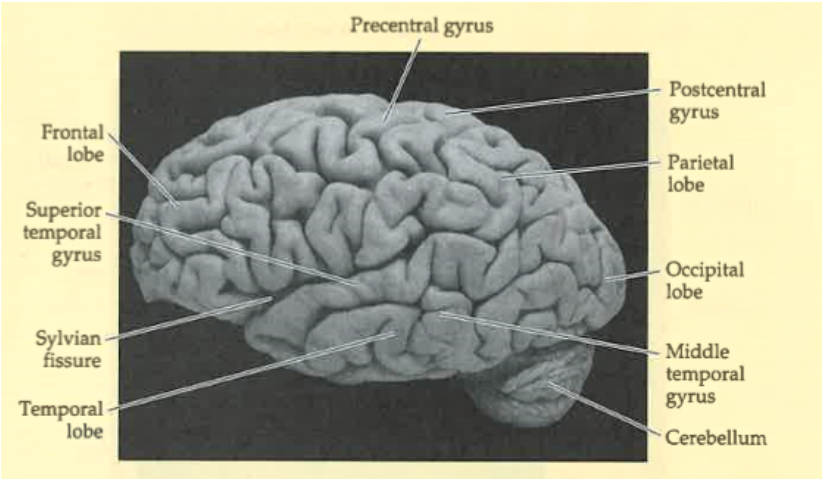

Figure A.2. Surface view of the human brain, LH [5].

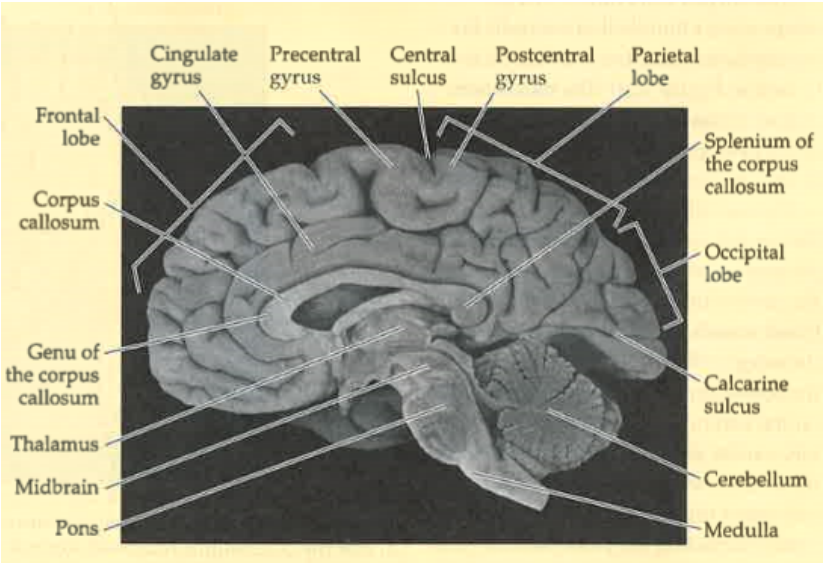

Figure A.3. Midsagittal view of the human brain, LH [5].

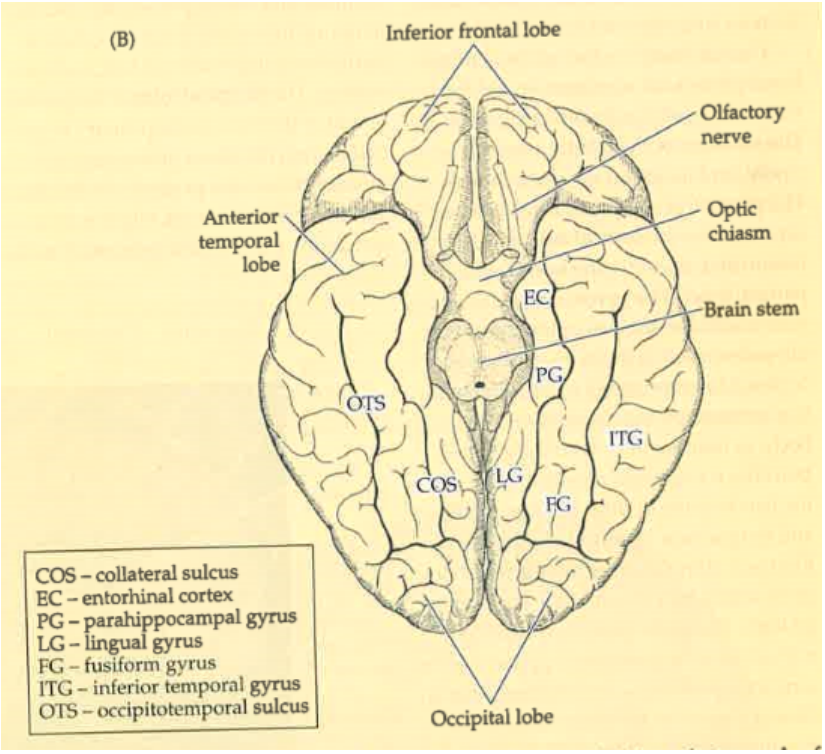

Figure A.4. Ventral view of the human brain, LH [5].